UAB
Universitat Autònoma de Barcelona

Dipòsit digital de documents de la UAB

This is the **accepted version** of the journal article:

Sorbelli, Leonardo; Azzarà, Beatrice; Cherin, Marco; [et al.]. «Why extant, why not extinct? A new extinct Latonia species (Anura: Discoglossidae) from the Early Pleistocene of the Apennine Peninsula provides clues on the survival of the genus in Eurasia». Journal of Systematic Palaeontology, Vol. 23, issue 1 (2025), art. 2554727. DOI 10.1080/14772019.2025.2554727

This version is available at https://ddd.uab.cat/record/321100

under the terms of the IN COPYRIGHT license

Why extant, why not extinct? A new extinct *Latonia* species (Anura; Discoglossidae) from the Early Pleistocene of the Apennine Peninsula provides clues on the survival of the genus in Eurasia

Leonardo Sorbelli[1,2,*], Beatrice Azzarà[3], Marco Cherin[3], Massimo Delfino[4,2], Zbynek Roček[5], Andrea Villa[2,*]

[1] Museum für Naturkunde, Leibniz Institute for Evolution and Biodiversity Science, Invalidenstraße 43, 10115 Berlin, Germany.

[2] Institut Català de Paleontologia Miquel Crusafont (ICP-CERCA), Edifici ICTA-ICP, c/ Columnes s/n, Campus de la UAB, 08193 Cerdanyola del Vallès, Barcelona, Spain.

[3] Dipartimento di Fisica e Geologia, Università degli Studi di Perugia, Via A. Pascoli, 06123, Perugia, Italy.

[4] Dipartimento di Scienze della Terra, Università degli Studi di Torino, Via T. Valperga Caluso 35, 10125 Torino, Italy.

[5] Department of Palaeobiology, Institute of Geology, Czech Academy of Sciences, Rozvojová 269, 16500 Prague, Czech Republic.

* Co-corresponding authors: leonardo.sorbelli@icp.cat; andrea.villa@icp.cat

Pietrafitta is one of the richest Early Pleistocene localities in the Italian Peninsula, and it hosts one of the latest occurrences of the discoglossid frog *Latonia* in Europe. This occurrence is here described as a new species. This new *Latonia* was a large frog, potentially feeding on hard invertebrates in the Pietrafitta palaeoswamp. Based on the first attempt at reconstructing phylogenetic relationships within *Latonia*, which we conducted here using a matrix with 20 taxa and 39 characters, the new Italian species is part of a still almost unknown clade that also includes *Latonia caucasica* from the Late Miocene of northern Caucasus. Almost all other extinct *Latonia*

species make up a second clade, represented in the fossil record from the Oligocene and including the youngest occurrence of the genus in Europe, from the Middle Pleistocene of Hungary. The only extant species, *Latonia nigriventer*, is the earliest branching taxon in our topology, but this could be due to its unique unsculptured morphology, which might be a secondary loss evolved during the Quaternary. The exostosis on cranial bones, which is considered a diagnostic feature of the genus, might have developed in the earliest *Latonia* in response to pronounced warming and drought. Later, starting after the Middle Miocene, this exostosis underwent a reduction process, possibly triggered by cooling, that led to Plio-Pleistocene forms sharing a narrower frontoparietal with a less pustular sculpturing. *Latonia dimenticata* is a clear example of this frontoparietal morphology. *Latonia nigriventer* may have further evolved a completely unsculptured morphology to face rapid environmental changes in the last Quaternary glacial phases and ultimately survive up to present day.

Keywords: Quaternary, Italian Peninsula, Europe, Middle East, *Latonia nigriventer*, exostosis

Introduction

The anuran discoglossid genus *Latonia* von Meyer, 1843 is of particular interest for several reasons. From a purely historical point of view, it is one of the earliest fossil frogs known to science, along with *Palaeobatrachus* Tschudi, 1838 and some other taxa whose identity remains unclear (e.g., *Palaeophrynos* Tschudi, 1838). The type species *Latonia seyfriedi* von Meyer, 1843 was described on the basis of a large articulated skeleton (estimated snout-vent length, SVL, measured from the anterior end of the premaxillary symphysis to the tip of the urostyle, can reach 20 cm) from the Middle Miocene deposits of the now defunct Öhningen quarry in southern Germany (von Meyer, 1843). This holotype specimen almost did not survive a bombing raid at the end of the Second World War in Karlsruhe. Due to the extraordinary large size of this frog, several other specimens from this type locality were purchased or donated as curiosities to other public and private collections, where they are still kept (e.g., Natural History Museum in London, Palaeontologisches Institut und Museum der Universität in Zürich, Teylers Museum in Haarlem). Syromyatnikova, Roček, et al. (2019) identified at least five individuals, but the exact number of specimens found in Öhningen is unknown.

The large size of *Latonia* was also the reason why this frog was relatively well known to palaeontologists in the 19th century. Among the isolated fossil bones recovered from various French sites of the Middle or Lower Miocene (e.g., La Grive St. Alban, Sansan, Laugnac), large cranial dermal bones with pustular or vermicular sculpturing have been found, such as frontoparietals and maxillae. Because of the sculpturing, they were for a long time not associated with *Latonia*, since all the skeletons of *Latonia* from Öhningen were exposed in ventral view and their cranial roof was embedded in matrix. However, even after the association of these disarticulated sculptured bones with *Latonia* was confirmed (on the basis of other skeletal elements; see Roček, 1994, for more details on historical *Latonia* material from France, attributed in the past to either *Latonia gigantea*

(Lartet, 1851) or *Latonia ragei* Hossini, 1993), another question was raised: is *Latonia* from Öhningen identical with *Latonia* from Sansan? This has only recently been resolved using modern, non-invasive techniques (Syromyatnikova, Roček, et al., 2019). It turned out that both bear sculpturing on their dermal bones and that diagnostic features can be found on other skeletal elements.

In recent years, knowledge of the stratigraphic and geographic distribution of *Latonia* has increased considerably. Remains of discoglossids referrable to this genus have been found in many localities of Western Palearctic spanning from Spain to Turkey, mostly recorded in Miocene layers (Roček, 1994; Rage & Roček, 2003; Vasilyan et al., 2019; Syromyatnikova, Georgalis, et al., 2019; Syromyatnikova, Tesakov, et al., 2019; Syromyatnikova et al., 2022 among others). The earliest frogs that can be undoubtedly assigned to the genus *Latonia* are from the late Oligocene of Vertaizon, France (i.e., *Latonia vertaizoni* (Friant, 1944)), and likely Kargı 1, Turkey (*Latonia* sp.; Vasilyan et al., 2019). Isolated large bones reported as *Discoglossus giganteus* Lartet, 1851 are known even from the middle Oligocene of Quercy (de Bonis et al., 1973; Rage, 1984), but Rage (2016) questioned the ability to identify Quercy discoglossids to genus rank. It has long been suspected that the Late Pliocene and Pleistocene distribution of *Latonia* shrank to the Mediterranean region and that this frog became extinct during the Pleistocene (Rage & Roček, 2003). Late Pliocene and Pleistocene *Latonia* were known from southern France, Hungary, Italy, Slovakia, and perhaps Ukraine (see summaries in Roček, 1994, 2013, and references therein). Works published in the last decades, however, showed that *Latonia* actually persisted during the Neogene and survived in the Quaternary (e.g., Vasilyan et al., 2014; Szentesi et al., 2019; Sorbelli et al., 2021), even as far north as western Germany with potential Late Pliocene relictual populations (Villa et al., 2024). The genus has recently been shown to survive in the Levant (Biton et al., 2013, 2016; Perl et al., 2017) as *Latonia nigriventer* (Mendelssohn & Steinitz, 1943), previously assigned to *Discoglossus*. Thus, this genus not only provides information on its anatomical evolution and phylogenetic

diversification over about 30 Myr against the background of changing paleogeography and climate, but also on its soft anatomy, which is so necessary for the interpretation of fossils.

Here we describe and formally establish a new *Latonia* species from the Early Pleistocene of Italy, based on fossil material from the locality of Pietrafitta previously reported as *Latonia* sp. in a recent article by Sorbelli et al. (2021). This discovery provides new evidence that more than one member of the genus *Latonia*—which disappeared from Western and Central Europe at the end of the Neogene—persisted in isolated populations within the Mediterranean and nearby refugia dated to the end of the Neogene and Pleistocene. Many of these surviving forms have previously been referred to under various names (e.g., *Archipelobates giganteum* Tatarinov, 1970; Chkhikvadze, 1981; *Discoglossus* cf. *giganteus*; Vergnaud-Grazzini, 1970; or *Pelobates robustus* Bolkay, 1913; Féjérváry, 1917) all of which are currently synonym of *Latonia* species or moved within *Latonia*. We further investigate the phylogenetic relationships of the new species within the genus using modern analytical techniques for the first time.

Geological setting

[Insert Fig. 1 here]

The palaeontological site of Pietrafitta (42°59’33”N, 12°12’42”E; Fig. 1) is located in central-western Umbria (Central Italy), about 15 km south of Lake Trasimeno. The site lies along the upper valley of the Nestore River within the Tavernelle-Pietrafitta Basins. These basins are referred to the Nestore synthem, within the Tiberino supersynthem. The Nestore synthem is divided into two subsynthems: the lowermost Tavernelle subsynthem and the uppermost Pietrafitta subsynthem. The latter, in the Early Pleistocene, was characterized by lacustrine/palustrine and alluvial plain conditions (Conti & Esu, 1981; Cherin et al., 2012; Pazzaglia et al., 2013). In the following phases

of the Pleistocene, tectonics caused an uplift of the area and the desiccation of the basin, with the establishment of the present-day fluvial environment of the Nestore River (Ambrosetti et al., 1989). At the edges of the Pietrafitta palaeolake, lignite deposition occurred within stagnant water sub-basins (Conti & Girotti, 1977; Ambrosetti et al., 1992, 1995; Gentili et al., 1996; Martinetto et al., 2014). Lignite layers are interbedded with thin clay layers bearing freshwater molluscs and oligohaline ostracods (Gliozzi et al., 1997), most likely coming from periodic high-energy events that have remobilized the bottom of the neighbouring lake. The overall thickness of the lignite beam is between about 5 and 8.5 m. Palaeobotanical data suggest that (1) the swampy area in which the lignite was formed was surrounded by broad-leaved deciduous forests under a humid climatic context and (2) a slight tendency towards a harshening of the climate can be detected from the bottom to top of the sequence (Ricciardi, 1961; Lona & Bertoldi, 1972; Martinetto et al., 2014, 2017).

During almost half a century of survey and excavations conducted in parallel with the industrial exploitation of the lignite (ca. 1950–1990), the site of Pietrafitta has yielded one of the richest vertebrate assemblages in the Italian Early Pleistocene, including some thousand specimens referred to at least 40 taxa of freshwater fishes, amphibians, reptiles, birds, and mammals (see updated faunal lists in Cherin et al., 2018; Sorbelli et al., 2021, 2023). The presence of several vertebrate skeletons in anatomical connection or slightly scattered and the overall sedimentological and taphonomic pieces of evidence, suggest a low degree of post-mortem displacement at Pietrafitta (Ambrosetti et al., 1992). The remains of the anurans were found during the extraction of the large vertebrate skeletons. Unfortunately, the lack of systematic excavation does not allow us to position precisely the fossils within the stratigraphic column. However, given the thickness of the lignite succession and the sedimentation rate estimated for this kind of brown coal deposits suggest a roughly isochronous deposition of the faunal and floral assemblages, furtherly confirmed by their taxonomic and taphonomic uniformity (Martinetto et al., 2014; Sorbelli et al., 2023 and references therein).The vertebrate assemblage is referred to the latest Villafranchian European Land Mammal

Age, in particular to the Farneta Faunal Unit, correlative with the late MNQ 18 biochron in the Mammal Neogene zones biochronological framework (approx. 1.6–1.4 Ma; Gliozzi et al., 1997; Gentili et al., 2000; Sorbelli et al., 2023).

Material and methods

Studied material and comparisons

The herein described new *Latonia* species is based on a sample of disarticulated bones found at Pietrafitta. At least some of these bones were found associated in disarticulated clusters isolated from other anuran bones (Fig. 1C), leading to the recognition of likely four different individuals. Bones referred to two main individuals were originally hosted in a plaster jacket after collection (each individual had its own plaster jacket; M.D., personal observation) and were later freed by one of the authors (M.D.). Attribution of all the bones found in each plaster jacket to a single individual is further supported by comparable size and absence of duplicated elements. On the other hand, size and duplication of elements suggest that at least two more individuals are represented in the additional isolated bones. A list of all the fossil bones, arranged per individual, is given in Supplemental Material Table 1. The studied material is stored at the Museo Paleontologico "Luigi Boldrini" in Pietrafitta, catalogued under six different repository numbers: SABAP_UMB 24.S241-4.1018 to SABAP_UMB 24.S241-4.1023. For the sake of simplicity, the code "S241-", which is invariable for each fossil, will be omitted from here on in the manuscript. The first two repository numbers are given to the two main individuals, whereas the other numbers refer to isolated bones that cannot be clearly associated to the former. Specific skeletal elements of the two main individuals are identified by a letter after the related main repository number (e.g., SABAP_UMB 24.4.1018a is the left premaxilla of SABAP_UMB 24.4.1018, whereas SABAP_UMB 24.4.1019m

refers to both scapulae of SABAP_UMB 24.4.1019; see Supplemental Material Table 1). These fossils were first briefly described in the unpublished PhD thesis of one of the authors (Delfino, 2002). A preliminary report was recently provided by Sorbelli et al. (2021), who provisionally referred them to *Latonia* sp. Preliminary inventory numbers (PFHER) reported by Sorbelli et al. (2021) are listed in Supplemental Material Table 1 along with the definitive ones used here throughout the text. Other previous brief reports of these fossils from Pietrafitta are by Ambrosetti et al. (1987; as *Bufo* sp.) and Rage & Roček (2003; as *Latonia* sp.).

The new species was compared to all known other species of *Latonia* based on both available literature (Špinar, 1978; Hossini, 1993; Roček, 1994, 2013; Rage & Hossini, 2000; Biton et al., 2016; Syromyatnikova & Roček, 2019; Syromyatnikova, Roček, et al., 2019) and personal observations. The anatomical nomenclature follows mainly Roček (1994), with additional terms from Sanchiz (1998a) and Syromyatnikova and Roček (2019). Structures on the ilia are named according to the revised terminology proposed by Gómez and Turazzini (2016). Anuran taxonomy follows Dubois et al. (2021). Measurements were taken with a digital calliper to the nearest 0.1 mm. Selected specimens were photographed with a Nikon D750 DSLR camera equipped with macro 1:1 lens Tamron SP AF 90 mm f/2.8.

Phylogenetic analysis

We conducted a phylogenetic analysis to preliminarily investigate relationships within discoglossids and in particular between extinct and extant *Latonia*. Our analysis is based on the morphological matrix published by Biton et al. (2013: supplementary table S2), with some modifications. The original *Latonia* Operational Taxonomic Unit (OTU) was replaced by separated OTUs for extinct *Latonia* species. The "*Latonia nigriventer* fossils" OTU was removed, because it was identical to *L. nigriventer* in all the scored characters, and investigating fossils attributed to this extant species is not a focus of our work. We also removed *Callobatrachus* Wang & Gao, 1999. This genus was

recently synonymised with *Liaobatrachus* Ji & Ji, 1998 by Dong et al. (2013), and its only species, *Callobatrachus sanyanensis* Wang & Gao, 1999, with *Liaobatrachus grabaui* Ji & Ji, 1998. Additionally, according to Dong et al. (2013), the morphology of the fossil assigned to *Callobatrachus* was originally misinterpreted and it is not related to discoglossids. We added all extinct *Latonia* species currently considered valid (type locality and age between parentheses), that is, *Latonia caucasica* Syromyatnikova & Roček, 2019 (Volchaya Balka, Russia; Late Miocene), *Latonia ragei* (Laugnac, France; Early Miocene), *Latonia seyfriedi* (Öhningen, Germany; Middle Miocene), *Latonia vertaizoni* (Vertaizon, France; late Oligocene), and the new species from Pietrafitta described herein, as well as the Middle Pleistocene *Latonia gigantea* (original attribution by Szentesi, 2019, but this species referral needs to be revised; see Discussion) from Esztramos 6 in Hungary (also known as Osztramos 6, but this spelling is incorrect for Esztramos Hill fossil localities according to Szentesi, 2019: p. 141). *Latonia gigantea* (Sansan, France; Middle Miocene) is here considered as a junior subjective synonym of *L. seyfriedi* following Syromyatnikova, Roček, et al. (2019), and it is thus not treated separately in the matrix. On the other hand, we scored *Latonia kolebabi* Špinar, 1976 (Ivanovce, Slovakia; Early Pliocene) as a separate OTU; this species was considered as a junior synonym of *L. gigantea* by Roček (1994), but we find value in treating it separately in our analysis to explore its relationships in the light of some features it shares with the new Pietrafitta species (see Discussion). We also added *Ascaphus* Stejneger, 1899 to use as outgroup. *Ascaphus* was the outgroup in most of Biton et al.'s (2013) analyses, but it was only coded for molecular data and was absent from the morphological-only matrix; because of this, the morphological scoring for this genus was made *ex novo* by us in this study. We further added 17 additional characters (C23 to C39), mainly focused on taxonomically significant features within *Latonia*. Therefore, our matrix is composed of 20 taxa and 39 characters.

The matrix was created with MorphoBank (O'Leary & Kaufman, 2012) and can be accessed together with the character list at the following link: http://morphobank.org/permalink/?P5094 [temporary review access, not to be shared without explicit permission from the authors: log in with

P5094; password LatoniaPietrafitta]. We revised Biton et al.'s (2013) scorings for characters 1 to 22 and scored the newly added characters based on literature and direct comparisons with specimens available in the collections of the Università degli Studi di Torino or on MorphoSource (https://www.morphosource.org/). Some of the specimens observed on MorphoSource were made available through the oVert project (Blackburn et al., 2024). Literature references and specimens used for scorings are reported in the respective taxon entry in the taxon list on MorphoBank. The analysis was performed in TNT v1.6 (Goloboff & Morales, 2023) as a New Technology Search, with 1000 trees in memory, all Use options selected and stabilizing consensus 5 times with a factor of 75. The branch collapsing option was selected. The New Technology Search was followed by a second round of tree bisection and reconnection. Trees were visualized using FigTree v1.4.4 (http://tree.bio.ed.ac.uk/software/figtree/).

Institutional abbreviations

MGPT MDHC - Massimo Delfino Herpetological Collection, Museo di Geologia e Paleontologia, Dipartimento di Scienze della Terra, Università degli Studi di Torino (Italy); PFHER - Pietrafitta Herpetofaunal Remains, Museo Paleontologico "Luigi Boldrini", Pietrafitta (Italy); SABAP_UMB - Soprintendenza Archeologia, Belle Arti e Paesaggio dell'Umbria (Italy).

Systematic palaeontology

Class **Amphibia** Linnaeus, 1758

Order **Anura** Duméril, 1805

Family **Discoglossidae** Günther, 1858

Genus ***Latonia*** von Meyer, 1843

Revised diagnosis. The following revised generic diagnosis can be proposed: 1) frontoparietal completely fused in the full-grown adult, but traces of a suture or a narrow, V-shaped fontanelle may be preserved on the anterior part of the ventral surface of the bone; 2) anterior and posterior parts of the incrassatio frontoparietalis unpaired; 3) pars contacta (a ridge in the frontoparietal articulating with the dorsolateral margin of the braincase) running from the lateral margin of the frontoparietal anterolateral process ("horn") posteromedially, then turning laterally onto the anterodorsal margin of the prootic; 4) dorsal surface of the frontoparietal covered by a pustular or ridge-like exostosis, which may extend laterally to varying degrees as the tectum supraorbitale over the anterior horn and prootic (however, exostosis absent in the extant *L. nigriventer* and the condition is unknown in Palaeogene species); 5) when the maxilla is covered by sculpture, exostosis mainly found on the posterodorsal part of the lateral surface, around the area of the processus zygomaticomaxillaris; 6) frontoparietal lacking foramina for the arteriae occipitales; 7) suture between the processus zygomaticomaxillaris and the lamella alaris of the squamosal straight; 8) palatine variably fused to the maxilla (as the processus palatinus); 9) angular bearing two processes, the processus paracoronoideus and the processus coronoideus; 10) presence of a distinct depression in the bottom of the sulcus pro cartilago Meckeli at the level of the processus coronoideus; 11) processus paraoccipitalis of the frontoparietal and corresponding crista on the posterior surface of the exoccipital prominent and mediolaterally compressed; 12) crista ventralis of the humerus paralleled distally by a shorter crista paraventralis; 13) caput humeri displaced laterally from the main axis of the bone, giving the humerus a distinctly asymmetrical shape in ventral view.

Latonia dimenticata sp. nov.

1987 *Bufo* sp. Ambrosetti et al.: 103.

2002 *Latonia* cf. *L. ragei* Delfino: 47, pl. 5, pl. 6A–F.

2003 *Latonia* sp. Rage & Roček: 157.

2021 *Latonia* sp. Sorbelli et al.: 562, figs 5–8.

Diagnosis. A species of the genus *Latonia*, the adults of which can be diagnosed by the following combination of characters: 1) maxillae unsculptured (Fig. 2B) ; 2) maxillary tooth row extending slightly beyond the processus pterygoideus (Fig. 2C); 3) frontoparietal and nasals covered by pustular exostosis; 4) frontoparietal narrow (Fig. 2G), without tectum supraorbitale extending into orbits; 5) pars contacta (Fig. 2I-J) poorly ossified, reaching the lateral margin of the frontoparietal posterolaterally; 6) prominentia ductus semicircularis posterioris very long (Fig. 2M); and 7) presence of a vertical and sigmoid ridge ventral to the prominentia ductus semicircularis posterioris, almost touching the occipital condyle (Fig. 2L).

In particular, *L. dimenticata* sp. nov. differs from *L. seyfriedi* (including the subjective junior synonym *L. gigantea*) in the unsculptured maxillae and the absence of tectum supraorbitale. It differs from *L. nigriventer* in the well-developed sculpturing on nasals and frontoparietal (Fig. 2E, G). It differs from *L. caucasica* and at least some specimens previously referred to *L. gigantea* (so now potentially belonging to *L. seyfriedi*, pending a revision of the specimens) in the posterior extension of the maxillary tooth row exceeding the level of the processus pterygoideus. It differs from *L. vertaizoni* in the well-developed processus coronoideus, longer than the processus paracoronoideus (Fig 3A), and from all other *Latonia* species, except some specimens of *L. ragei*, in having a processus coronoideus inclined posterolaterally. It differs from *L. caucasica*, *L. nigriventer*, *L. ragei*, and at least some specimens previously attributed to *L. gigantea* (so now potentially *L. seyfriedi*) in the very long prominentia ductus semicircularis posterioris. It differs

from at least some specimens attributed to *L. gigantea* (again, currently potentially referrable to *L. seyfriedi*) in the presence of a posterior vertical ridge on the prooticooccipitals, and from *L. caucasica* in the sigmoid shape and greater length of said ridge.

Derivation of name. The species name comes from "dimenticata" (adjective, Italian for "forgotten"). This refers to the fact that the description of this new species has been overlooked and then somehow forgotten for more than 20 years since the original description by Delfino (2002). At the same time, the species is an apparently isolated remnant of a clade that was once very successful in Europe, but by the time the Pietrafitta fossils were deposited, was almost exclusively represented on the continent by these last, isolated survivors that were "forgotten behind" by their siblings during their retreat eastward.

Common name. We suggest the following common names for the new species: Apennine painted frog (English); latonia appenninica (Italian).

Holotype. SABAP_UMB 24.4.1019 (Figs 2–6), a partial disarticulated skeleton including both maxillae, the right nasal, the frontoparietal, the left prooticooccipital, both angulars, the atlas, one presacral vertebra, three ribs, the urostyle, both coracoids, both scapulae, the left humerus, both radioulnae, both ilia, both femora, both tibiofibulae, the ?right tibiale, the ?right fibulare, one metatarsal, five phalanges, and four other indeterminate bone fragments that were collected in the same cluster with the other bones. Relevant measurements are provided in Table 1.

[Insert Figs 2-6 starting from here]

Paratypes. SABAP_UMB 24.4.1018 (Figs 7–12), a second partial disarticulated skeleton (including the left premaxilla, both maxillae, the frontoparietal, both pterygoids, the parasphenoid, both prooticooccipitals, both angulars, the atlas, several fragments of presacral vertebrae, four ribs, the urostyle, the left coracoid, both scapulae, both clavicles, both humeri, both radioulnae, both ilia, the ischium, both femora, both tibiofibulae, the ?right tibiale, and several indeterminate bone fragments found in association with the other elements); SABAP_UMB 24.4.1020 (Fig. 13A–D), a right prooticooccipital; SABAP_UMB 24.4.1021 (Fig. 13E–F), a left humerus; SABAP_UMB 24.4.1022 (Fig. 13G–J), associated ?right tibiale and fibulare; SABAP_UMB 24.4.1023, one metatarsal. Relevant measurements are provided in Table 1.

[Insert Figs 7-13 starting from here]

Type locality and age. Pietrafitta quarry (coordinates: 42°59'33"N, 12°12'42"E), Umbria, Italy; Early Pleistocene (1.6–1.4 Ma; MNQ 18), late Villafranchian (Farneta Faunal Unit) (Gliozzi et al., 1997; Gentili et al., 2000; Sorbelli et al., 2023).

Description

The bones belong to four different, large individuals. In the cases of SABAP_UMB 24.4.1018 and SABAP_UMB 24.4.1019, the bones were found together in the same isolated cluster. A few other elements were found isolated. Among these, the prooticooccipital SABAP_UMB 24.4.1020, smaller than those of the two main individuals, supports the presence of a third individual. The presence of a fourth individual is suggested by a pair of tibiale and fibulare, SABAP_UMB 24.4.1022, whose size is comparable to those of the two main individuals, and therefore cannot belong to the same animal as the isolated prooticooccipital. In fact, the isolated tibiale and fibulare represent the largest individual recovered from Pietrafitta, followed by SABAP_UMB 24.4.1019,

SABAP_UMB 24.4.1018, and finally the individual represented by the isolated prooticooccipital SABAP_UMB 24.4.1020. Selected measurements are reported in Table 1.

Premaxilla (Fig. 7A–B). SABAP_UMB 24.4.1018a is the only available premaxilla. It is almost complete and characterised by a narrow pars facialis, with a deep recessus marsupiatus on its inner lateral side (Fig. 7B). The dorsal part of the pars facialis is broken off. The lamina horizontalis is narrow and the pars palatina (sensu Roček, 1994), which is a posteriorly-directed projection on the medial side of the lamina, is rounded (Fig. 7A). The external surface of the bone is smooth. The dental row consists of 13 tooth positions, housing teeth that are not completely preserved but have the same morphology as in the maxilla (see below).

Maxilla (Figs 2A–D; 7C–F). The maxillae are clearly characterised by a smooth lateral surface without any sculpturing (Figs 2B, D; 7D, F). The only observable irregularities are areas of slightly exfoliated surfaces and the presence of small foramina often associated with short, shallow and straight furrows. The anterior half of the two best preserved maxillae (belonging to SABAP_UMB 24.4.1019; Fig. 2A–D) has a wide but shallow longitudinal groove on the external surface. In general, only the tooth bases are preserved. The teeth are pedicellated, pleurodont and densely packed, curved and pointed. The maximum total tooth height (including the pedicle and measured in medial view) is about 1.2 mm. The crista dentalis is not very long, ending slightly posterior to the deep lamina horizontalis and the processus pterygoideus (Figs 2A, C; 7C, E). It is possible to estimate the maximum number of tooth positions from the best-preserved maxillae to about 35 per maxilla. As in other *Latonia*, the anterior end of the maxilla is toothless, probably indicating an extensive overlapping suture with the premaxilla. The medial surface of the maxilla is marked by a wide posterior depression below the processus zygomaticomaxillaris (Figs 2A; 7C). The processus pterygoideus is large and extends both posteriorly and medially. The area corresponding to the processus palatinus is broken in all maxillae. The processus posterior is long and tapers distally (Figs 2B).

Nasal (Fig. 2E–F). SABAP_UMB 24.4.1019b is the only preserved nasal. This has been previously confused with a frontoparietal fragment, reported as PFHER00034B by Sorbelli et al. (2021). The nasal is not complete. It preserves only the sculptured posteromedial part of the bone, whereas the paraorbital and anterior processes and the thin anterolateral (parachoanal) margin are missing. The medial margin of the bone, representing the medial suture between the two nasals, is straight. On the ventral surface, a low but distinct ridge defines an anterolateral concavity. The dorsal sculpturing consists of densely packed tubercles that are weakly coossified with the underlying bone, suggesting secondary coossification. The posterior end of the bone projects slightly into a small smooth area, probably for contact with the frontoparietal.

Frontoparietal (Figs 2G–J; 7G–H). All frontoparietals are fragmentary, but clearly indicate that the bone was unpaired and narrow, covering only the braincase and not extending onto the orbits. The best-preserved frontoparietal is SABAP_UMB 24.4.1019c (Fig. 2G–J), even though it is broken into three different fragments. Together, these fragments represent most of the anterior half of the bone as well as its posterior portion. An undetermined portion of the middle part is missing. On the other hand, only the posterior end of the frontoparietal SABAP_UMB 24.4.1018c (Fig. 7G-H) is preserved, being broken anteriorly at a level slightly more posterior than the posterior fragment of SABAP_UMB 24.4.1019c. SABAP_UMB 24.4.1019c undoubtedly belongs to an adult individual as evidenced by the well-developed dorsal pustular sculpturing, the well-developed incrassatio frontoparietalis, and its size (Fig. 2G, J). SABAP_UMB 24.4.1018c is slightly smaller than the other frontoparietal, has a distinctly rough facies dorsalis devoid of the secondary coossified sculpturing, and the margins of the posterior part of the incrassatio frontoparietalis are slightly less marked (but this may be a preservation artifact, given that these margins are badly preserved and signs of breakage are visible; Fig. 7G). The dermal sculpturing on the frontoparietal (as clearly observed in SABAP_UMB 24.4.1019c) consists of small tubercles that fuse with one another in the anterior section, forming low, anterolaterally oriented and irregular ridges bounding straight grooves. The sculpturing is not coossified with the underlying bone surface.

Ventrally, the incrassatio frontoparietalis is composed of two well-separated surfaces: the anterior one (preserved only in SABAP_UMB 24.4.1019c; Fig. 2I–J) is narrow and elongated, whereas the posterior one is shorter and rhomboid. Lateral to the anterior portion of the incrassatio frontoparietalis, ventral to each anterolateral horn, the surface contacting the sphenethmoid is characterized by sharp ridges that are confluent toward the posterior half of the fragment. At least in SABAP_UMB 24.4.1019c, the anterolateral margins of the rhomboidal posterior part of the incrassatio are closely bordered by a poorly developed ridge, which diverges posterolaterally towards the edge of the bone. This ridge represents the posterior end of the pars contacta, where the frontoparietal joins the dorsal margin of the braincase (Fig. 2I, J). In the anterior portion of the frontoparietal of the same specimen, the pars contacta is represented by a rather sigmoid and well-developed ridge, splitting from the vertically folded lateral margin of the bone anteromedially, but then turning back towards the ventral surface of the anterolateral horns, where it disappears. The ventral surface of the frontoparietal posterior to the incrassatio frontoparietalis is the contact surface with the tectum synoticum (dorsal surface of both prooticooccipitals).

The anterolateral corners of SABAP_UMB 24.4.1019c diverge and bear two incomplete, small horns, the right one of which is better preserved (Fig. 2G). There is no sign of interdigitation with the nasals and no tectum supraorbitale. The absence of this tectum appears natural, and not related to breakage. Because of this, the frontoparietal appears slender in dorsal view. By the posterior end of the frontoparietals, the facies dorsalis is arched posteriorly in SABAP_UMB 24.4.1019c (Fig. 2H) and ends in a straight margin in SABAP_UMB 24.4.1018c (Fig. 7H). Due to the limited posterior extent of the facies dorsalis, the smooth and sloping posterior surface of the bone is exposed dorsally. A distinct median crest is visible in the middle of this surface in SABAP_UMB 24.4.1019c (Fig. 2H), whereas SABAP_UMB 24.4.1019c only shows an indistinct median hump (Fig. 7H). The sloping posterior surface of the frontoparietal is bounded laterally by the paraoccipital ridges, which run from the posterolateral corners of the facies dorsalis to each processus paraoccipitalis (Figs 2H; 7H). The ridges are parallel to the median crest in

SABAP_UMB 24.4.1019c and diverge posterolaterally in the other frontoparietal. The paraoccipital processes are shorter in SABAP_UMB 24.4.1019c (only the right one is preserved; Fig. 2H, J) and more developed in SABAP_UMB 24.4.1018c (Fig. 7G, H). The longer processes of the latter specimen imply that its paraoccipital ridges continue well beyond the margins of the bone. The posterior margin of the frontoparietal (margo occipitalis) between the paraoccipital processes is gently arched, with a small but distinct processus posterior in the middle.

Pterygoid (Fig. 7I–L). Both pterygoids of SABAP_UMB 24.4.1018 are preserved and almost complete. This element has a long ramus maxillaris, which is narrow in dorsal/ventral view but distinctly expands towards the anterior end in medial/lateral view (Fig. 7J, L). The rami posterior and interior are broken off in both pterygoids. A well-developed ventral flange (also called dilatatio alaris, sensu Bolkay, 1919, by Biton et al., 2016) is present on the lateral side of the bone, and it bears visible rugosities on its dorsal surface (Fig. 7J, L). A deep and narrow sulcus pterygoideus extends on the dorsal surface of the pterygoid, passing medial to the ventral flange and on the lateral surface of the ramus maxillaris (Fig. 7J, L). The ventral surface of the pterygoid is smooth (Fig. 7I, K).

Prooticooccipital (Figs 2K–N; 8; 13A–D). All prooticooccipitals are large and robustly built. In all fossils, the prootic and exoccipital components are tightly fused, with no evidence of a cartilaginous suture between the two capsular components on the medial wall of the otic capsule. The crista parotica is prominent dorsolaterally and widens distally (Figs 2L; 8F; 13B). The distal end of the crista is forked to originate a shorter processus prooticus rostralis brevis (sensu Špinar, 1978) anteriorly and a longer processus prooticus caudalis longus (sensu Špinar, 1978) posteriorly (Figs 2M, N; 8C; 13C). Despite the potential presence of some minor damage (Fig. 8G), this forked condition is not an artifact of preservation, as clearly shown by the well-preserved crista parotica of SABAP_UMB 24.4.1019d (Fig. 2M, N) and the comparable morphology figured by Biton et al. (2016, fig. 2A) for an adult of *L. nigriventer*. In life, the crista parotica was in contact with the

ramus paroticus of the squamosal, but it was not extensively overlapped by the latter (the articulation surface is reduced to a small area on the dorsal surface of the bifid lateral end; Figs 2M; 8G; 13C). The contact area for the frontoparietal (facies prootico-parietalis) is striated and delimited by a sharp ridge (Figs 2M; 8C, G; 13C). On the anterior surface of the bone, there is a distinct and broad palatoquadrate contact area (called the anterior prootic ridge by some authors; e.g., Špinar, 1978; Hossini, 1993), which lies ventral to a deep sulcus venae jugularis (Fig. 2K; 8A, E; 13A). This sulcus is continuous medially with the foramen prooticum, whereas laterally it turns posteriorly below the base of the crista parotica. On the ventral surface of the prooticooccipital is the canal for the hyomandibular branch of the facial (VII) nerve, which is partially bridged by a bone (Fig. 2N; 8D, H; 13D). It should be noted that this canal is located on the ventral surface of the bone in *Latonia* (Figs 2N, 8D, 8H, 13D), whereas in *Leiopelma* Fitzinger, 1861 it is located on the lower part of the anterior surface of the prootic (Stephenson, 1951). The condylus occipitalis is tear-shaped and rather prominently surmounted by the prominentia ductus semicircularis posterioris. The latter is laminar; it narrows posteriorly and extends far beyond the condyle in dorsal view (i.e. in the best preserved prooticooccipital, the prominentia surpasses the condyle by half of its length in dorsal view; Fig. 2M–N). In posterior view, a sharp, low and more-or-less sigmoid ridge starts from the lateral margin of the prominentia and runs ventrally, ending at the level of the lateral corner of the condylus occipitalis (Figs 2L; 8B, F; 13B). A narrow groove separates the end of the ridge from the condyle. Lateral to the ventral end of the vertical ridge, a triangular and laminar process can be either present (e.g., in SABAP_UMB 24.4.1019d; Fig. 2L) or absent (e.g., in SABAP_UMB 24.4.1020; Fig. 13B). The presence of this process is variable even in a single individual: in SABAP_UMB 24.4.1018, as a matter of fact, it is present on the left prooticooccipital (Fig. 8F), but not on the right one (Fig. 8B).

Angular (Fig. 3, 9). The largest and best-preserved angular, i.e. SABAP_UMB 24.4.1019e (Fig. 3A–D), has a preserved length of 37.3 mm. However, as the anterior tip is missing, the original total length was probably at least 40 mm. Based on a comparison with the large specimens of *L.*

seyfriedi, this would correspond to a skull length of about 45 mm, and thus to a SVL of about 150 mm. Each angular (Figs 3; 9) has two processes: the anterior processus paracoronoideus, which has a long base but is less prominent in dorsal view, and the posterior processus coronoideus, which can vary in size (Figs 3A, E; 9A, E). The processus paracoronoideus bears transverse ridges on its dorsal surface, which define furrows of variable depth. In medial view, the dorsal contour of this process is markedly concave (more concave in SABAP_UMB 24. 4.1019 than in SABAP_UMB 24.4.1018). The processus coronoideus is always well developed and inclined posteromedially. In dorsal view, the sulcus pro cartilago Meckeli has a sigmoid course (Figs 3C, G; 9C, G). It has a constant depth anteriorly, but deepens posteriorly, at the level of the processus coronoideus. At the posterior end of the bone, the sulcus widens considerably, giving rise to the extremitas spatulata (Figs 3A, E; 9A, E). The lateral surface of the bone bears a deep, elongated depression, which is bounded by sharp cristae both dorsally and ventrally. The ventral one of these cristae is the crista mandibulae externa.

Atlas (Fig. 4A–F). A complete atlas (SABAP_UMB 24.4.1019g; Fig. 4A–F) and a fragmentary atlantal centrum (SABAP_UMB 24.4.1018h) were recovered. Other parts of the atlas of SABAP_UMB 24.4.1018 may be present among the several fragments of vertebrae attributed to this individual (SABAP_UMB 24.4.1018i). The centrum of the atlas of *L. dimenticata* sp. nov. is dorsoventrally depressed and has a subcircular posterior cotyle and two anterior cotyles, which are mediolaterally elongated and dorsolaterally inclined, not confluent in the middle (cervical cotylar type II sensu Lynch, 1969). The spatium interglenoidale is narrow. The median ridge (crista ventralis) is strongly marked on the ventral surface of the atlantal centra, as in other *Latonia* species (Fig. 4B). A low carina neuralis runs in the midline of the dorsal surface of the neural arch, from the anterior margin to the tip of the robust and posterodorsally projecting processus spinosus (Fig. 4A, D).

Presacral vertebra (Fig. 4G–L). A single, almost complete presacral vertebra (SABAP_UMB 24.4.1019h) is present, with only the distal part of the right transverse process and the left prezygapophysis broken off. It is robust, with an opisthocoelous centrum and strong, posteriorly inclined transverse processes. The left process is almost complete, indicating that it was short and slightly expanded distally (Fig. 4G). The zygapophyses are broad and elliptical. The carina neuralis is a rounded but distinct ridge that extends beyond the level of the postzygapophyses with a posterior point, which is however broken off (Fig. 4H). Several fragments of vertebrae belonging to SABAP_UMB 24.4.1018, including at least four isolated centra and various fragments of neural arch, were also found, but they are too poorly preserved to add significant morphological information.

Rib (Fig. 10A). All ribs have slightly widened ends and are therefore narrower in the middle. The largest rib bears a hooked uncinate process arising from the dorsal surface of the bone. One rib was found still articulated with a small fragment of the related transverse process.

Urostyle (Figs 4M; 10B–E). In lateral view, the urostyle is moderately convex dorsally. Anteriorly, there are two fossae condyloideae for the bicondylar articulation with the sacral vertebra (Fig. 10B). The two fossae are closely juxtaposed and only slightly mediolaterally elongated. They coalesce in the middle in SABAP_UMB 24.4.1019j, but not in SABAP_UMB 24.4.1018m. At the level of the canalis coccygeus, there is a pair of short transverse processes, which are flattened dorsoventrally, inclined posterolaterally and rounded at their end (Fig. 10C). The canalis coccygeus is wide and circular (Fig. 10B). A narrow midline fissure (a feature present in discoglossids; Roček, 1994; Biton et al., 2016; Villa et al., 2021) crosses the rounded carina neuralis, but it is partially closed in the intermediate section (Figs 4M; 10C). The carina lowers in the posterior part of the bone, which is simply rounded. No additional processes or horizontal laminae extending posteriorly from the transverse processes were seen. Ventral to the transverse processes, on both sides of the urostyle, there is a posterior opening of the intervertebral canal (Fig. 10E).

Scapula (Figs 5C–F; 11C–D). The right scapula of SABAP_UMB 24.4.1018 (Fig. 11C, D) is almost complete, whereas the preservation is worse in the two scapulae of SABAP_UMB 24.4.1019 (Fig. 5E–D) and even more in the left one of SABAP_UMB 24.4.1018 (which only preserves a fragment of the lateral end). The bone is relatively short mediolaterally (almost squared in overall view) and robust. The lateral end (pars suprascapularis) is slightly wider than the medial end (pars glenoidalis plus pars acromialis) (Figs 5E; 11C). The partes acromialis and glenoidalis are of approximately equal size and separated by a deep and narrow sinus interglenoidalis (Fig. 11C). A very well developed tenuitas cranialis is present on the margo anterior, contributing to the squared appearance of the scapula (Fig. 11D). The margo posterior, on the other hand, is markedly concave and without ridges. Both the dorsal and ventral surfaces of the bone are smooth.

Coracoid (Fig. 5A–B; 11A–B). Of the three preserved coracoids, only SABAP_UMB 24.4.1019l (Fig. 5A–B) is complete. The two others, SABAP_UMB 24.4.1018n (Fig. 11A–B) and SABAP_UMB 24.4.1019k (not figured), are broken at the base of the intumescentia glenoidalis and do not preserve the flat and fragile pars epicoracoidealis. The lateral end (pars glenoidalis), which articulates with the scapula, is large and slightly flattened or subcircular in cross section, whereas the medial end (pars epicoracoidealis) is dorsoventrally depressed (Figs 5A; 11A). Viewed dorsally, both ends are approximately equal in width, at least in the best-preserved specimen (Fig. 5A). The main body of the coracoid, as far as can be said from the complete one, is elongated, narrow and straight in dorsal/ventral view. The anterior margin is regularly concave, whereas the posterior one is straight.

Clavicle (Fig. 11E–H). There are only two fragmentary clavicles (SABAP_UMB 24.4.1018q), both missing the distal portion of the extremitas medialis. They are rather slender and strongly curved. An elongated concavity at their lateral end served to articulate with the pars acromialis of the scapula. The sulcus cartilagine praecoracoreidealis is deep and well defined (Fig. 11F, H).

Humerus (Figs 5G–J; 11I–L; 13E–F). Both humeri of SABAP_UMB 24.4.1018 are preserved in very good conditions (Fig. 11I–L). On the other hand, SABAP_UMB 24.4.1019 only preserves the two ends of the left humerus (SABAP_UMB 24.4.1018n) as isolated fragments (Fig. 5G–J). SABAP_UMB 24.4.1021 is represented by the distal half of a left humerus only (Fig. 13E–F). The humeri have a straight shaft. They are slightly curved laterally in their distal part, resulting in a lateral displacement of the spherical caput humeri, a poorly developed epicondylus radialis, the distal margin of which is confluent with the outline of the caput, and a robust epicondylus ulnaris (Figs 5G, I; 11I, K; 13E). The crista ventralis is well developed, flared laterally in its most prominent segment, and flanked by a lower crista paraventralis (Figs 5G, D; 11I, K). The crista medialis is either prominent or moderately developed, a feature potentially associated with sexual dimorphism (Fig. 11J, L). The crista lateralis is lower, but still distinct (Fig. 11I, L). The fossa cubitalis ventralis is shallow (Fig. 11I, K). The olecranon scar is narrow and elongated. In extant discoglossids (i.e., *Discoglossus* Otth, 1837), the caput humeri is completely ossified and spherical in adults, whereas the proximal epiphysis remains cartilaginous (Púgener & Maglia, 1997). A similar, spherical and well ossified caput humeri, together with the general robustness and the size, support adulthood for these humeri from Pietrafitta.

Radioulna (Figs 5K–M; 11M). Both radioulnae of SABAP_UMB 24.4.1019 are preserved and complete (the right one, SABAP_UMB 24.4.1019o, is figured in Fig. 5K–M), whereas only fragments of those of SABAP_UMB 24.4.1018 are available (the right one, SABAP_UMB 24.4.1018t, is figured in Fig. 11M). A bone fragment herein identified as the proximal end of the left radioulna of SABAP_UMB 24.4.1018, labelled as SABAP_UMB 24.4.1018s (not figured), was originally mistaken for a fragment of coracoid by Sorbelli et al. (2021). The radioulnae have a narrow collum antebrachii and widen strongly distally, so that their distal end is considerably wider than the proximal one (Figs 5L; 11M). The olecranon is rather prominent (its maximum length is slightly more than half of the maximum width of the proximal end of the radioulna; Fig. 5M). A well-ossified olecranon, such as the one visible in the fossils from Pietrafitta, is another adult

feature in extant discoglossids (Púgener & Maglia, 1997: fig. 5). The distal end is rather flat in distal view (Fig. 5K). In the same view, the radial part of the distal end has a wider cross section, whereas the ulnar part is slightly smaller and more depressed.

Ilium (Figs 6A–E; 12A–E). The most complete ilium is the left one of SABAP_UMB 24.4.1018 (Fig. 12A–B). All other elements are more fragmentary, with the right one of the same individual preserving only the iliac body (Fig. 12C–E) and the left one of SABAP_UMB 24.4.1019 only the shaft (Fig. 6A–B). The right one of SABAP_UMB 24.4.1019 is split into two fragments, including the iliac body (Fig. 6C–E) and the shaft (not figured) respectively, which were treated as separated bones by Sorbelli et al. (2021). The ilia have a well-developed dorsal crest on their shaft and an extensive and rather laterally swollen dorsal tubercle, which is continuous with the dorsal outline of the crest anteriorly and with the proximal, anterodorsally oriented part of the shaft posteriorly (Figs 6C; 12A, B). As a result, the shaft emerges anterodorsally from the iliac body, but at the level of the tubercle, it bends anteriorly and its anterior part is almost straight. A separate tubercle that would protrude from the dorsal surface of the shaft is not developed, but ventral to the dorsal tubercle is a shallow and barely distinguishable depression (called the fossula tuberis superioris by Roček, 1994; tubercular fossa sensu Gómez and Turazzini, 2016; Figs 6C; 12A, C). The ilium presents an elongated dorsal acetabular expansion (pars ascendens sensu Roček, 1994) that terminates in a point (Figs 6D; 12B, C). The ventral acetabular expansion (pars descendens sensu Roček, 1994) is shorter and rounded (Figs 6D; 12C). Due to the anterodorsal orientation of the proximal portion of the iliac shaft and of the dorsal tubercle and the posterodorsal prominence of the dorsal acetabular expansion, the dorsal margin of the iliac body is concave, with a rather wide angle. The acetabular fossa lies almost entirely on the ilium, with only a small posterior part extending onto the cartilaginous pubis and the anterior part of the ischium (Figs 6A; 12A, C). A shallow supraacetabular fossa is present (Figs 6C; 12A, C). On the medial surface of the iliac body, there is a deep interiliac groove (Fig. 12B, D). The interiliac tubercle is strongly reduced, difficult to recognise.

Ischium (Fig. 12F). Only one ischiadic component of the pelvis is available: SABAP_UMB 24.4.1018v. Although both ischia are fused together, they were articulated to the ilia by cartilage, as evidenced by well-preserved articular margins for the dorsal ilioischiadic juncture. Only the ventral part articulating with the cartilaginous pubis seems to be incomplete. Thus, from the reconstruction of this almost complete, robust and subelliptical bone, the ischium complex was rather short anteroposteriorly and it hosted a small contribution to the acetabular surface.

Femur (Figs 6F–G; 12G). The femora are long and slender. Most are complete, except for the right one of SABAP_UMB 24.4.1018. In a comparable way to other anuran femora, they are sigmoid, with a low but distinct crista femoris present on the proximal half of the bone, although not extending to the end (Figs 6G; 12G).

Tibiofibula (Figs 6H–K; 12H–K). All tibiofibulae are complete. They are slightly longer than the respective femora. In SABAP_UMB 24.4.1018 (Fig. 12H–K), the femur/tibiofibula length ratio is 0.93 for the only pair of bones for which it can be calculated; in SABAP_UMB 24.4.1019 (Fig. 6H–K), the ratio is either 0.94 (left side) or 0.95 (right side). Similar to the femora, the tibiofibulae are long and slender bones. They are straight and slightly expand toward the ends. The ends have a similar width, only slightly larger distally. A low but relatively sharp crista cruris is present (Figs 6H; 12I). The sulci distalis and proximalis are deep (Figs 6H; 12H). The elliptical tibial and fibular elements at the ends of the bone have parallel long axes (as in other discoglossids; Bailon, 1999).

Tibiale and fibulare (Figs 6L–M; 13G–J). A couple of tibiale (Fig. 6L) and fibulare (Fig. 6M) from SABAP_UMB 24.4.1019, possibly the right ones, were found in good preservation conditions. Only the proximal fragment of the possible right tibiale of SABAP_UMB 24.4.1018 (not figured) is preserved. Another pair, SABAP_UMB 24.4.1022, including a complete potential right tibiale (Fig. 13I–J) and the proximal half of the related fibulare (Fig. 13G–H) is available, not belonging to either of the above-mentioned individuals. The tibiale and fibulare are not fused; the former is slightly larger than the latter. Both are long and slender, with expanded ends. The distal end of the

tibiale is larger than the distal end of the fibulare, whereas the proximal ends are of about the same size. In both bones, the proximal end is larger in cross section than the more laminar distal end. On the ventral surface of the proximal end of the tibiale, a low ridge occurs along the lateral margin.

Metatarsal. A single metatarsal of SABAP_UMB 24.4.1019 is preserved. It is very long and slender, with an enlarged proximal end. The distal end is broken off. In medial and lateral views, it is clearly bent ventrally. A small fragment of the proximal end of another metatarsal belonging to an indeterminate individual, SABAP_UMB 24.4.1023, is also available.

Phalanx (Fig. 6N–O). The phalanges are also slightly curved ventrally and slightly grooved along the ventral surface. No distal phalanx is preserved.

Other bones. Several fragments of other bones can be referred to either SABAP_UMB 24.4.1018 or SABAP_UMB 24.4.1019 because of spatial association at the time of recovery in the field, but they are in too bad of a preservation status to give additional morphological information. Among others, these include a small portion of the parasphenoid of SABAP_UMB 24.4.1018, which is not described above because of the little morphological information it provides.

Phylogenetic analysis

[Insert Fig. 14 here]

The first run of our phylogenetic analysis resulted in 864 trees with 62 steps. The Strict Consensus Tree (SCT; not shown in the figure) was completely unresolved, with a huge polytomy in the ingroup. Because of this, we decided to run a second iteration, deactivating all OTUs with less than 50% of the characters scored (a reduced matrix without these OTUs can be found in the Documents section of the MorphoBank project related to this work). This led to the deactivation of five OTUs,

mainly Cretaceous taxa but also the Miocene *Latoglossus* Hossini, 2000 and *L. vertaizoni*. The latter species is part of the clade our analysis was focused on (i.e., *Latonia*), but it came out as one of the most problematic taxa in the matrix. This is likely because of poor knowledge of its cranial anatomy leading to several missing scorings in our matrix, which is mainly focused on cranial characters. Thus, we decided to still deactivate it. Results of this second iteration include four most parsimonious trees, 60 steps long. The SCT (Fig. 14A) is more resolved than in the first iteration, but a polytomy is still present at the node including bombinatorids, alytids, and discoglossids. Looking at the resulting trees, this polytomy is mainly caused by: 1) *Barbourula* Taylor & Noble, 1924 placed as sister to discoglossids in one tree out of four (vs sister to *Bombina* Oken, 1816 in a monophyletic Bombinatoridae Gray, 1825 in all other trees); 2) the unstable position of *Eodiscoglossus* Villalta, 1954 and *Wealdenbatrachus* Fey, 1988 (in a clade sister to either alytoids or *Alytes* Wagler, 1829, or as consecutive sister taxa to discoglossids). The most common placement for the two Mesozoic taxa is as consecutive sister taxa to discoglossids (two out of four trees), with *Eodiscoglossus* always diverging first. Given this degree of uncertainty, we decided to run a third iteration of the analysis, further deactivating *Eodiscoglossus* and *Wealdenbatrachus*. This iteration resulted in a single, almost completely resolved tree (Fig. 14B), with a length of 54 steps. The only unresolved node is at the base of discoglossids. A fourth and fifth iteration, run to test the effects of deactivating only one of *Eodiscoglossus* and *Wealdenbatrachus*, are presented in Supplemental Material File 1.

Except for the first one, the topology inside *Latonia* is consistent throughout all iterations (including the fourth and fifth ones; see Supplemental Material File 1). *Latonia nigriventer* is the earliest branching species, sister to a clade with developed exostosis on cranial bones. This latter clade is composed of two subclades: one with *L. caucasica* and *L. dimenticata* sp. nov., and another one with *L. ragei* and an additional subclade with *Latonia* with sculptured maxillae. In the latter, the Esztramos 6 *Latonia* (referred to *L. gigantea* by Szentesi, 2019) is sister to *L. seyfriedi* + *L. kolebabi*.

Discussion

A new *Latonia* species from Pietrafitta

In their study of the ectothermic vertebrates from the Pietrafitta lignite deposits, Sorbelli et al. (2021) already recognised the peculiarity of the *Latonia* fossils from the site, suggesting their potential pertinence to an unknown species within the genus. Nevertheless, they provisionally refrained from formally erecting a new species, pending more detailed comparisons. Here, we provide such comparisons and further discuss the differences and similarities between the *Latonia* remains from Pietrafitta and those attributed to the *Latonia* species so far described. These data sustain Sorbelli et al.'s (2021) claim for a new taxonomic status for the Pietrafitta fossils, which we describe here as *Latonia dimenticata* sp. nov.

The sculpturing on cranial bones has always played a major role in the taxonomic history of *Latonia*, both at the genus and species rank. As a matter of fact, the development of such sculpturing as a separated exostosis is used as a clear distinctive feature discriminating *Latonia* from other anurans with sculptured skulls (e.g., pelobatids; Roček, 1994, 2013). When it comes to different species within the genus, the most significant information concerns which skull bones are sculptured, and which are not. In *Latonia*, sculpturing may be present on the maxillae, the nasals, the frontoparietal, and the squamosals. According to the current knowledge about *Latonia* species, sculptured maxillae are characteristic of *L. seyfriedi* (including *L. gigantea* following Syromyatnikova, Roček, et al., 2019, and thus also *L. kolebabi* following Roček, 1994), whereas maxillae of other known species, including the extant *L. nigriventer* and *L. dimenticata* sp. nov. from Pietrafitta, have a smooth lateral surface. Nasals are sculptured in *L. caucasica*, *L. dimenticata* sp. nov., and *L. seyfriedi* (unknown in *L. kolebabi*). Of the five specimens of *L. nigriventer* studied

by Biton et al. (2016), only the largest one available to the authors displayed a very faint sculpturing on the nasals. There are no nasals attributed to *L. ragei* and *L. vertaizoni*. Generally, *Latonia* has a sculptured frontoparietal, and *L. dimenticata* is no exception. The condition is unknown for *L. vertaizoni*, whose frontoparietal is not preserved in the holotype and only known specimen (Roček, 1994). The material referred to *L. ragei* by Hossini (1993) does not include frontoparietals either, but Sanchiz (1998b) identified sculptured frontoparietals from Austria as pertaining to this species (together with a wealth of other cranial and postcranial bones). The report of a sculptured frontoparietal for *L. ragei* by Syromyatnikova and Roček (2019) is based on this occurrence. The identification of the Austrian material was based on the presence of smooth maxillae, given that back then *L. ragei* was the only species within the genus known to display such a feature. However, more recent works highlighted the existence of other *Latonia* species with unsculptured maxillae (see above). Therefore, the specific identity of the Austrian material studied by Sanchiz (1998b) should be revised, and we here consider the actual condition displayed by the frontoparietal in *L. ragei* as uncertain for the time being. The frontoparietal of *L. nigriventer*, on the other hand, clearly is devoid of sculpturing (Biton et al., 2016). The absence of preserved squamosals in the sample of *Latonia* remains from Pietrafitta hinders any evaluation of the potential sculptured or unsculptured condition for these bones in *L. dimenticata* sp. nov., as well as any comparisons with other species.

The morphology of the sculpturing itself on the frontoparietal was also included in the original diagnosis for *L. gigantea* proposed by Rage & Hossini (2000, p. 195), as: “Face dorsale du frontopariétal ornée de petits tubercules disposes sans ordre dans la partie postérieure et moyenne, mais organisés en crêtes irrégulières et divergentes vers l’avant dans la partie antérieure” (Dorsal surface of frontoparietal sculptured with small tubercles arranged with no order on the posterior and middle parts, but organized in irregular and anteriorly-divergent ridges on the anterior part). It has to be noted that the authors themselves treated their diagnosis as only preliminary, mainly pending further data on *L. seyfriedi* (later provided by Syromyatnikova, Roček, et al., 2019, through the use of micro-computed tomography on a topotypic specimen). As a matter of fact, the mentioned

sculpture morphology is shared by all species for which a sculptured frontoparietal is known, and thus it likely represents a more general feature of the genus *Latonia* as a whole. In at least *L. seyfriedi* (again including *L. gigantea* as well), the sculptured surface of the frontoparietal (facies dorsalis) widely extends laterally to create a very well-developed tectum supraorbitale by each side of the bone. Roček (1994, p. 735) highlighted that this structure is ontogeny-dependent, with younger individuals having narrower frontoparietals because the tectum developed with growth. In *L. dimenticata* sp. nov., the tectum is absent in the large SABAP_UMB 24.4.1019 (the individual with the best preserved frontoparietal), thus in contrast with adults and more like juveniles of *L. seyfriedi*. Nevertheless, all other evidence (large size, strong degree of ossification) points to adulthood for this individual, meaning that the absence of a developed tectum could be a significant feature to distinguish the new species when compared to *L. seyfriedi*. Heterochrony may be involved in the evolution of this morphology, given the similarity with the young specimens of the other species. Evaluation of this feature is impossible for species for which the frontoparietal is unknown, of course, and it is problematic for *L. caucasica* as well. Only posterior portions of frontoparietals are available in the material referred to this species, moreover, pertaining to small animals. In these fossils, the preserved portion of the facies dorsalis is narrow (Syromyatnikova & Roček, 2019, p. 501). On the unsculptured frontoparietal of *L. nigriventer*, the facies dorsalis does not develop laterally at all, being only present as a narrow strip in the middle of the dorsal surface of the bone (Biton et al., 2016, fig. 3D).

On the medial side of the maxillae, the posterior extension of the tooth row is considered as another significant taxonomic character for *Latonia* species. In *L. nigriventer*, *L. ragei*, and *L. dimenticata* sp. nov., the row extends slightly beyond the processus pterygoideus, whereas it ends at the level of the process in *L. caucasica*. In the maxillae referred in the past to *L. gigantea* (now *L. seyfriedi*), the character is variable, and it may end or not beyond it. This cannot be evaluated for *L. vertaizoni* and the holotype of *L. seyfriedi*, but the row seems to extend posteriorly in a topotypic specimen of the latter species (Syromyatnikova, Roček, et al., 2019, fig. 5f). When it comes to the morphology of

the processus coronoideus on the angular, *L. dimenticata* sp. nov. shares a well-developed process with all other species but *L. vertaizoni*. This process is directed posteromedially (extended posteriorly in the words of Syromyatnikova and Roček, 2019) in *L. dimenticata* sp. nov. as it is in most specimens of *L. ragei*. Other remaining species have a medially extending processus coronoideus (note that this is unknown for topotypic material of *L. seyfriedi*, whose condition is retrieved by the material previously assigned to *L. gigantea*). The latter condition is also displayed by some *L. ragei*, but it is rare in this species (Rage, personal communication reported by Syromyatnikova and Roček, 2019).

A very peculiar feature displayed by *L. dimenticata* sp. nov. is the rough dorsal surface of the ventral flange of the pterygoids. However, only very few fossil pterygoids are known for *Latonia*, and so this character is of little use for comparisons for the time being. Nevertheless, the ventral flange is smooth in *L. nigriventer* and in a single pterygoid from the Late Miocene of Catalonia attributable to *L. seyfriedi* (originally referred to as *L. gigantea*; Villa et al., 2019). The well-developed and rugous ventral flange of the pterygoid might imply some degree of dietary specialization in *L. dimenticata* sp. nov. A mainly durophagous diet was suggested by Biton et al. (2016) for *Latonia* based on osteological features and the gut content of a scanned specimen of the extant *L. nigriventer*. This feeding habit may also apply to *L. dimenticata* sp. nov., due to shared osteological features used by Biton et al. (2016) to sustain their hypothesis (e.g., presence of two processes on the angular, thickened upper margin of the posterolateral wall of the angular, strong articulations of skull elements). Dietary specialization might have been even taken to a stronger extent in *L. dimenticata*, given the peculiar morphology of the pterygoid ventral flange. This flange acts as a guide for the lower jaw in *Barbourula* (Roček et al., 2016) and could thus be involved in the feeding strategy of the animal. The morphology of the flange in *L. dimenticata* sp. nov. clearly differs from the smooth one in *L. nigriventer* and the fossil pterygoid from Catalonia, but more recently similar pterygoids were found in an Early Pliocene assemblage with *Latonia* from Greece (Georgalis et al., 2024). What this really means in terms of functional anatomy cannot be

confidently stated at the moment, but it seems that it was a shared feature at least in some Pliocene and Pleistocene *Latonia*. Living habits and feeding strategies of extinct *Latonia* are still a poorly investigated topic, but they are clearly worthy of further scrutiny.

Potentially, the most diagnostic bone in *L. dimenticata* sp. nov. is the prooticooccipital. As it is the case in all *Latonia*, it bears a strong prominentia ductus semicircularis posterioris. However, this structure extends beyond the occipital condyle for about half of its total length in the species from Pietrafitta, being way longer than it is in *L. caucasica*, *L. nigriventer*, *L. ragei*, and at least some specimens previously attributed to *L. gigantea* (e.g., a left prooticooccipital from La Grive-St. Alban figured by Roček, 1994, fig. 5A). In the holotype of *L. seyfriedi*, on the other hand, the length of the prominentia is more comparable to the condition seen in the Pietrafitta specimens. On the posterior surface of the prooticooccipital of *L. dimenticata* sp. nov., a vertical ridge is present, running ventrally to end almost in contact with the occipital condyle. This ridge takes a roughly sigmoid shape. A possible homologue of this ridge is present in *L. caucasica*, but it is straighter and well separated from the condyle in this species (Syromyatnikova & Roček, 2019, fig. 2c-2). A prooticooccipital previously referred to *L. gigantea* figured by Roček (1994, fig. 5A), and thus potentially referrable to *L. seyfriedi* under the current proposed synonymy, does not show the presence of a similar ridge. Because of the mode of preservation (i.e. as articulated and fragmentary specimens on slabs), the presence and possible shape of a vertical ridge cannot be evaluated for the type material of *L. seyfriedi*. This further holds true for *L. vertaizoni* as far as all prooticooccipital features are concerned. Both a very long prominentia ductus semicircularis posterioris and a sigmoid vertical ridge approaching the condyle on the posterior surface are present on the prooticooccipital of another species: *L. kolebabi* from the Pliocene of Slovakia. This species was later considered as a junior subjective synonym of *L. gigantea* by Roček (1994), and the material should be thus referred to as *L. seyfriedi* following the recent taxonomic statements by Syromyatnikova, Roček, et al. (2019). However, the prooticooccipital morphology displayed by these Slovakian fossils suggests that it might be interesting to reevaluate them after the new state of

knowledge. A detailed approach to such revaluation is out of the scope of the present study, but it is worth comparing the type material of *L. kolebabi* with the one of *L. dimenticata* sp. nov. In addition to the similarities in the prooticooccipital, the two species share the sculptured frontoparietal and the well-developed processus coronoideus. However, the latter process is not posteromedially directed in *L. kolebabi* (Špinar, 1978, fig. 67). Moreover, the Slovakian species has sculptured maxillae and a developed tectum supraorbitale, in contrast to *L. dimenticata* sp. nov. The tectum seems to be less developed in *L. kolebabi* than in other *Latonia*, resulting in a narrow frontoparietal that was one of the main diagnostic characters proposed by Špinar (1978). However, Roček (1994) stated that the tectum seems just to be damaged, hence the apparent narrower frontoparietal morphology. In any case, the tectum is clearly present (Špinar, 1978, fig. 64), thus differing from the *Latonia* from Pietrafitta.

The postcranial morphology is more homogenous within *Latonia*, with very few characteristics differing sufficiently to bear taxonomic significance among species. The shape of the sacral transverse processes and their inclination compared to the main axis of the sacral vertebra are the only postcranial features used to discriminate *Latonia* species (see diagnoses in e.g., Roček, 1994, 2013; Syromyatnikova & Roček, 2019). However, sacral vertebrae are missing from the available material of *L. dimenticata* sp. nov., and these features are thus of no use in this discussion. On the other hand, we were able to calculate the femur/tibiofibular length ratio for at least SABAP_UMB 24.4.1018 and SABAP_UMB 24.4.1019 of *L. dimenticata* sp. nov., and to compare it with at least one other species, *L. seyfriedi*. The ratio for the latter species is reported to be about 0.9 by Roček (1994, 2013), and thus it does not seem to differ substantially from the one observed in *L. dimenticata* sp. nov. (0.93-0.95). Hindlimbs of *L. vertaizoni* are too badly preserved to allow calculating the ratio, whereas we have no measurements available for *L. nigriventer*. The other extinct species are all represented by isolated remains, which were not found in association. Because of this, their femur/tibiofibular length ratio cannot be calculated.

Taking all of this into account, we consider that the *Latonia* remains from Pietrafitta differ enough from other known species within the genus to allow the description of a new one. This species inhabited at least one locality in the central part of the Italian Peninsula during the Early Pleistocene. It is interesting to note that the only other known European Pleistocene occurrence of *Latonia*, the Middle Pleistocene one from Esztramos 6 reported by Szentesi (2019), clearly pertains to a different species. Attributed to *L. gigantea* by the above-mentioned author, the Hungarian remains include a maxilla with a rough lateral surface (reported as "secondary sculpture" by Szentesi, 2019, p. 146), a prooticooccipital with a short prominentia ductus semicircularis posterioris and no vertical ridge posteriorly (at least based on what can be observed in figures 8 and 9 by Szentesi, 2019), and an angular with a very little developed processus coronoideus (Szentesi, 2019, fig. 12). All these features distinguish this occurrence from the Pietrafitta one. However, the tectum supraorbitale of the Hungarian frontoparietal appears undeveloped (Szentesi, 2019, figs 6, 7), similar to the condition observed in *L. dimenticata* sp. nov. It is unclear whether this may stem from a juvenile/subadult condition of the fossil from Esztramos 6, from a breakage, or even from the presence of another species with a narrow frontoparietal in the European Pleistocene. The Esztramos 6 *Latonia* is also worth further investigations, therefore, possibly with the aid of additional material from the several fossil localities of the Esztramos Hill.

Phylogenetic relationships of *Latonia* species

The analysis we performed for this study is meant only as a first approach at the phylogeny of *Latonia* using modern computational tools, to be further expanded in the future. As a matter of fact, a larger taxon and character sampling might prove useful to understand more clearly the relationships of *Latonia* with other extinct frogs, which were proposed as potential alytoid or discoglossid relatives in previous works (such as those originally included in our matrix, but deactivated during the analysis). In particular, it would be useful to increase the number of

postcranial characters, given that our matrix is mostly focused on cranial ones (only 12 out of 39, ~30% characters are scored on postcranial elements). Postcranial characters could be important to better resolve the relationships of *L. vertaizoni*, whose postcranial morphology is better known than the cranial one. However, it has to be noted that postcranial interspecific variation is considered to be low in *Latonia*, based on the current available knowledge. This could pose an intrinsic limit on our potential understanding of *L. vertaizoni*, pending the recovery of additional fossils with better preserved skulls. Furthermore, some of Biton et al.'s (2013) original characters we used may be modified or at least reworded in future analyses (see character list in MorphoBank), allowing for better computation of the osteological variation between these animals by the software. In any case, relationships within *Latonia* in the different iterations of our analysis remain constant, meaning that some inferences can be discussed based on the topology resulting from our dataset, especially regarding the extinct species of the genus.

The most unexpected result is probably *L. nigriventer* being the earliest diverging species, despite being the only extant *Latonia*. Assuming that this species originated in the area, this would imply a very long gap in the eastern history of *Latonia* (contrary to what has been reported so far in the literature on the basis of the absence of pre-Pleistocene fossil record; Gardner & Rage, 2016), given that separation of the lineage leading to *L. nigriventer* would have happened before the origin of all species described based on European material. An alternative, probably more likely explanation for the placement of *L. nigriventer* in the tree topology, however, could be its nature as the only (almost) completely unsculptured *Latonia* species currently known (Biton et al., 2016). Indeed, this condition, which may be a secondary loss developed as an adaptation to Quaternary environmental changes (see next section in the Discussion), excludes *L. nigriventer* from the subclade including all other *Latonia* OTUs (except the deactivated *L. vertaizoni*), which is supported by two exostosis-related synapomorphies (i.e., sculpturing present on nasals and frontoparietal; see apomorphy list in Supplemental Material File 1). *Latonia nigriventer* itself does not present unambiguous autapomorphies. Further data and fossils, together with the anticipated discovery of extinct *Latonia*

species related to *L. nigriventer* in pre-Quaternary Middle East are needed in order to better understand the relationships of this species. Remains attributed to *L. nigriventer* are available from Pleistocene localities in the same valley where the extant species lives nowadays (Biton et al., 2013, 2016, 2019, 2021) and *Latonia* fossils are known from the Oligocene to the Pleistocene of Turkey (Vasilyan et al., 2014, 2019; Syromyatnikova, Georgalis, et al., 2019; Syromyatnikova, Tesakov, et al., 2019; Syromyatnikova et al., 2022), thus opening the possibility of future discoveries about the evolution of Middle Eastern painted frogs. Expanding the phylogenetic matrix with additional characters may also be of help, lowering the weight that exostosis-related characters have in our analysis.

The two main subclades within the extinct/sculptured *Latonia* clade are supported by prooticooccipital and vertebral synapomorphies, respectively. The new Italian species, *L. dimenticata* sp. nov., clusters with the Late Miocene *L. caucasica* from northern Caucasus due to a long prominentia ductus semicircularis posterioris and the presence of a vertical ridge on the posterior surface of the prooticooccipital. However, both these characters are shared with at least some members of the other subclade, i.e. *L. kolebabi* (both characters) and at least some *L. seyfriedi* (the long prominentia). Moreover, the prominentia in *L. dimenticata* sp. nov. is much longer than it is in *L. caucasica*, and the shape of the vertical ridge is different in the two species. The other subclade, on the other hand, is supported by a single synapomorphy: posterolaterally inclined anterior margins of the sacral transverse processes. This is indeed different from the condition seen in *L. nigriventer* and *L. caucasica*, in which the margins are perpendicular to the main body axis, but the state of the character is unknown in *L. dimenticata* sp. nov. and variable in *L. seyfriedi*. Separation of *L. ragei* from the other OTUs within the subclade is explained by the absence of maxillary exostosis in the former. Sculptured maxillae were long considered as a diagnostic feature of *L. gigantea* (e.g., Rage & Hossini, 2000; Roček, 1994, 2013), and indeed the two other OTUs included within this subclade of *Latonia* with sculptured maxillae were either referred to such species (the Esztramos 6 *Latonia*; Szentesi, 2019) or considered as a junior subjective synonym of it

(*L. kolebabi*; Roček, 1994). Following the recent taxonomic statement by Syromyatnikova, Roček, et al. (2019), all these occurrences would be now referred to as *L. seyfriedi*, and this agrees with them clustering together with the *L. seyfriedi* OTU in our analysis. However, some differences are indeed present among them, implying some potential complexity in the taxonomy within the subclade: the *Latonia* from Esztramos 6 potentially presents a lower development of the tectum supraorbitale than both *L. seyfriedi* and *L. kolebabi*, whereas *L. kolebabi* differs from *L. seyfriedi* in the presence of a sigmoid vertical ridge on the posterior surface of the prooticooccipital. This further highlights the need of additional work on fossil *Latonia* to comprehend its infrageneric diversity. Pending more data and a new revision of the fossils, we refrain from presenting formal proposals on the taxonomic status of the different OTUs included in the subclade with sculptured maxillae, but this subclade may be preliminary defined as a *L. seyfriedi* complex for operational purposes (e.g., to assign fossil maxillae preserving exostosis recovered in fossil assemblages).

Overall, the resulting topology in our analysis for the extinct species of *Latonia* suggests origins from two different lineages for the latest survivors of the genus in Europe, that is, *L. dimenticata* from the Early Pleistocene of Pietrafitta and the *Latonia* from the Middle Pleistocene of Esztramos 6. The latter would be part of a lineage documented in the fossil record since the late Oligocene (material of *L. ragei* from Coderet described in the original paper by Hossini, 1993; see also Roček, 1994, 2013), which was widespread all over Europe throughout the Neogene (and had representatives in Anatolia as well; Syromyatnikova et al., 2022). The new Italian species, on the other hand, seems more related to a species from the Late Miocene of the Caucasus, thus hinting towards a potential ghost lineage that separated from the other one early in the evolutionary history of *Latonia* and is known to us only from an isolated Miocene occurrence at the border with western Asia and its last representative in the Pleistocene of Italy. Interestingly, neither of these two European clades would be closely related with the only extant species, which may have been derived from its own lineage potentially developing in the Middle East. Of course, it is possible that a closer relationship of the extant *L. nigriventer* with either one of these clades is masked in our

topology by its derived, unornamented morphology. For sure, this indicates that much still must be done to clarify the evolutionary history of *Latonia*.

The development of cranial exostosis as a potential adaptive trait for *Latonia*

Current knowledge of the geographic and stratigraphic distribution of *Latonia* comes from a relatively large number of sites in Europe and the Middle East (Biton et al., 2013, fig. 4), ranging from the early Oligocene (MP 21; Rage, 2016) to the Recent, although some of these finds were taxonomically misinterpreted as *Pelobates* Wagler, 1830 or *Discoglossus* and later referred to *Latonia* only because of their large size. In the meantime, the diagnostic characters of the genus have been refined on the basis of both articulated and disarticulated skeletons, which means that the distribution data will also be more accurate.

If comparisons are based on the frontoparietal alone as one of the main diagnostic elements, the most striking feature is that all, with the exception of *L. vertaizoni* and other Oligocene representatives in which the frontoparietal is not known, have some form of exostosis. All articulated skeletons of the Miocene *L. seyfriedi* from Öhningen were preserved in ventral aspect, so the dermal cranial roof is embedded in matrix, but micro-CT scanning revealed that both the frontoparietal, the posterior part of the maxillae, the nasals, and the lamella alaris of the squamosal were covered by a dense pustular exostosis, which in the frontoparietal is arranged anteriorly and to a lesser extent also laterally in ridges, and protrudes laterally as an extensive tectum supraorbitale with nearly straight orbital margin (Syromyatnikova, Roček, et al., 2019). A similarly ornamented frontoparietal is known from the Middle Miocene of Sansan (e.g., Roček, 1994, fig. 7F; Syromyatnikova, Roček, et al., 2019, fig. 2).

Pliocene occurrences of *Latonia* show the same type of pustular to ridge-like sculpturing, but the tectum supraorbitale is much less extensive, which is also reflected by distinctly concave orbital

margins. This holds true for the frontoparietals from Esztramos 1 (= Osztramos 1; MN 14, northern Hungary; Venczel, 2001, fig. 1a) and Ivanovce (MN 15, Slovakia; types of *L. kolebabi*; Špinar, 1978, pls. 64a–b, 65a–c), although in the Esztramos 1 fossil the pustular exostosis appears to be largely worn out. In the Early Pleistocene material from Pietrafitta, the frontoparietals seem to have the pustular exostosis mainly reduced to a tiny, granular type, both on the frontoparietal and nasals (Figs 2E, 2G–H), but completely absent on the maxillae (Figs 2B, 2D, 7D, 7F). Note that the fragment of frontoparietal of SABAP_UMB 24.4.1018 (slightly smaller than the frontoparietal of SABAP_UMB 24.4.1019, but still rather large) seems to miss the pustular exostosis, but still presents a rough facies dorsalis. Besides, the frontoparietals from Pietrafitta are narrow, with the tectum supraorbitale extremely reduced or absent and the facies dorsalis narrower posteriorly than anteriorly. The same type of the frontoparietal with a posteriorly narrow facies dorsalis without any exostosis (only presenting a coarse surface of the facies dorsalis) comes from the Lower Pleistocene Pasinler Beds, Erzurum Province, north-eastern Turkey (Vasilyan et al., 2014). Although the posterior part of the frontoparietal reported by Vasilyan et al. (2014, fig. 5 a1–a3) undoubtedly belongs to *Latonia*, a presumed anterior portion referred to the same taxon (Vasilyan et al., 2014, fig. 5 a4–a5) is less unequivocal.

The frontoparietal from the Middle Pleistocene site Esztramos 6 reported by Szentesi (2019) corresponds to other Early Pleistocene *Latonia* (i.e. *L. dimenticata* and the Pasinler Beds occurrence mentioned above) in the narrow posterior part of the facies dorsalis, the absence of the tectum supraorbitale, and the deeply concave orbital margin. Nevertheless, it still bears a pustular exostosis, although it is absent along the lateral margins and sparse in its posterior part (Szentesi, 2019, figs 6, 7). Based on what can be seen in Szentesi's (2019) fig. 4, the associated maxilla is completely devoid of exostosis, as in other known Pleistocene *Latonia*, even though a rough texture with isolated tubercles is visible on the lateral surface ventral to the processus zygomaticomaxillaris. Recent adult *L. nigriventer* have a frontoparietal that is narrow posteriorly

but broad anteriorly, lacks a tectum supraorbitale, and has only a narrow, elevated portion of bone along the midline that can be considered a vestigial facies dorsalis (Biton et al., 2016, figs 2A, 3D).

Comparison of the Pleistocene *Latonia* and extant *L. nigriventer* with Miocene and Pliocene forms suggests that one of the main evolutionary trends was the loss of the exostosis on the facies dorsalis of the fused frontoparietals and, judging from a rudimentary frontoparietal fontanelle indicating their incomplete fusion in the most recent *Latonia*, an abbreviated ontogeny (paedomorphosis). It can be assumed that if ontogeny could continue, the fontanelle would be closed and the bony structures arising in the superficial layer of the skin (epidermis or cutis), generally known as osteoderms, but here in the form of pustules, would fuse with the underlying dermal bones (frontoparietal, maxilla, nasal, and the lamella alaris of the squamosal), which arise earlier, in the deeper layer of the skin (dermis). Such epidermal pustular exostoses may even arise in the skin independently of the dermal bones (Duellman & Trueb, 1986, fig. 14–5B). Exostoses are often associated with hyperossification and are not uncommon in anurans (Evans et al., 2014).

The reasons for the presence of epidermal exostosis in anurans are poorly understood and are mostly attributed to the prevention of evaporative water loss in arid or seasonally dry environments (e.g., Seibert et al., 1974; Paluh et al., 2020). This explanation is supported by observations on extant, unrelated *Ceratophrys* Neuwied, 1824 and *Pyxicephalus* Tschudi, 1838, which inhabit warm, dry, non-forested environments with ephemeral pools (see discussion in Evans et al., 2014). These conditions may also apply to the environmental preferences of *Latonia*, the earliest representatives of which appeared in the Oligocene, particularly after an abrupt and pronounced warming around 26 Ma (late Oligocene Warming of Zachos et al., 2001, fig. 2) that led to comparatively warm mean annual temperatures and dry climate in the late Oligocene and Early Miocene.

Frontoparietals (or other potentially sculptured elements of the skull roof) are currently unknown in early *Latonia* species with smooth maxillae, but the evolution of the sculpturing pattern can be

tracked in slightly younger time periods. Subsequently, exostosis development in Neogene and Quaternary *Latonia* can be more clearly correlated with temperature. The warm phase started at the Oligocene/Miocene transition peaked during the late Middle Miocene Climatic Optimum (~16.9 to 14.7 Ma; Steinthorsdottir et al., 2021, and references therein), and it was followed by a gradual cooling with increasing amplitude of climatic fluctuations. This trend continued until the Early Pliocene (~6 Ma), but the cooling intensified in the Late Pliocene and Pleistocene. The deterioration of climatic conditions seems to be reflected in a gradual reduction of the frontoparietal exostosis. The representatives of *Latonia* from around the Middle Miocene Climatic Optimum, such as adult *L. seyfriedi* from the Middle Miocene (Astaracian) of Öhningen, had a frontoparietal with extensive tectum supraorbitale and completely covered by dense pustular exostosis (Syromyatnikova, Roček, et al., 2019, figs 5C, 5D). Similarly extensive was the exostosis on the Middle Miocene *Latonia* frontoparietals from Sansan (Syromyatnikova, Roček, et al., 2019, figs 2A–B), which have a comparable age to those from Öhningen, and Hambach 6C (Villa et al., 2024, fig. 13I–J), which are slightly older (Orleanian). *Latonia* from the Late Miocene (Vallesian) of Hrytsiv (also spelled as Gritsev) had a moderately reduced tectum (Roček, 2019, figs 5J–M). *Latonia caucasica* from the Late Miocene (Turolian) of Volchaya Balka in southern Russia was comparatively even more reduced, so that in its posterior part it did not extend beyond the facies dorsalis (Syromyatnikova & Roček, 2019, figs 2a–b), as in Pliocene representatives.

In most of the Pliocene forms, the tectum does not extend beyond the lateral and posterior margins of the facies dorsalis, giving the frontoparietal a narrow, anteriorly divergent shape, as in the Early Pliocene (MN 14) *Latonia* from Esztramos 1 (Venczel, 2001, fig. 1A). In *L. dimenticata* sp. nov. from the Early Pleistocene of Pietrafitta and *Latonia* sp. from the Pasinler Beds in Turkey (Vasilyan et al., 2014, figs a1–a3), the posterior part of the facies dorsalis shows no sign of a tectum, so it is very narrow posteriorly. The same is true for the Middle Pleistocene *Latonia* from Esztramos 6 (Szentesi, 2019, figs 6, 7). Thus, it can be concluded that in the period between the Middle Miocene and the Middle Pleistocene, characterised by a cooling from the temperatures of the Middle

Miocene Climatic Optimum at about 15 Ma (mean annual temperature 18.4 °C, about 3 °C higher than today; You et al., 2009) to the temperatures of the Late Pleistocene (33–12 ka), when surface air temperatures in the eastern part of Central Europe were 2-9 °C colder than today (Kovács et al., 2012), the extent of pustular exostoses on the frontoparietal decreased from a size extending well into the orbit and over the otic capsule on both sides of the cranium to a size not exceeding laterally the width of the facies dorsalis (or that of the braincase between the otic capsules). Interestingly, this represents a reversed relationship with pluviometry and aridity, with occurrences presenting the most developed exostosis found during the wetter Middle Miocene Climatic Optimum and a reducing trend following the climatic deterioration driven by the late Cenozoic glacial cycles.

The trend towards a reduction in the extent of the exostosis was accompanied by a concomitant trend for the high and well-defined pustules to become less prominent and even partially absent on some parts of the facies dorsalis. This trend was delayed compared to the reduction in the extent of the exostosis, and its final stage can be characterised by a complete absence of exostosis, so that the dorsal surface of the bone is only rugose (Venczel, 2001, fig. 1A; Vasilyan et al., 2014, fig. 5a1). However, although such a reduction in the pustularity of the exostosis undoubtedly existed in the Pleistocene, it can be confused with damage caused by fossilization conditions, as the exostosis can be partially or completely destroyed during fossilization. In addition, the development of exostoses depends on the age of the individual, i.e. they are moderately developed in juveniles and more developed in adults.

While it seems that the reduction of the frontoparietal exostosis can be satisfactorily correlated with the deterioration of the climate between the Middle Miocene and the Middle Pleistocene (more precisely, the older phase of the Middle Pleistocene according to Janossy and Kordos, 1977), *Latonia* from the cool Middle Pleistocene (about 0.5 Ma) of Esztramos 6 is clearly different from the extant *L. nigriventer*. The latter differs not only in the complete loss of the exostosis and the extreme reduction of the facies dorsalis, but also in the incomplete fusion of the frontoparietals,

suggesting an abbreviated ontogeny due to paedomorphosis. Adults of the Miocene and Plio-Pleistocene *Latonia* all have a firmly fused frontoparietal, with no trace of a median suture.

It is clear that the pronounced frontoparietal changes that characterised *L. nigriventer* had to occur within a very short period of time during the Late Glacial. The Pleistocene cooling, with an increase in the amplitude of global climate variations between cold glacials and warmer interglacials, undoubtedly had a serious impact on the behaviour and distribution of ectothermic amphibians. Following the Last Glacial Maximum (22–19 ka), the global ice volume decreased by about 10% within a few hundred years, which was undoubtedly associated with profound climatic changes (Anderson et al., 2007). The last glacial cold period, the Younger Dryas, ended abruptly 10.7 ka with a sudden rise in temperature (a 7 °C warming in South Greenland was completed in about 50 years; Dansgaard et al., 1989). Sudden drops in temperature, followed by similarly sharp rises in temperature, were undoubtedly associated with the drying out of the ponds. A comparatively short time before (0.5 Ma), palaeobatrachids became extinct, albeit for other reasons related to their living habits of permanent water dwellers (Wuttke et al., 2012). Anurans may respond to even transient climate warming leading to drying water bodies by shortening the period of larval development. *Discoglossus pictus* Otth, 1837 can complete larval development from fertilised egg to end of metamorphosis in 20 days under laboratory conditions, but the froglets are tiny and incompletely ossified (Z.R., personal observations). This may have been a way for *Latonia* to cope with sudden temperature increases at the end of the Younger Dryas and during the Holocene, leading to the current potentially paedomorphic morphology of the only extant species.

Conclusions

[Insert Fig. 15 here]

Latonia remains from the Early Pleistocene of Pietrafitta, previously suggested to represent a new species within the genus (Sorbelli et al., 2021), are here confirmed to represent a new taxon, which is formally described as *Latonia dimenticata* sp. nov. (Fig. 15). The new species significantly documents the osteology of one of the last surviving populations of these painted frogs in Europe prior to their extirpation, thanks to the finding of at least two individuals preserving a large part of their bones plus some additional, isolated skeletal element potentially referable to two further individuals. *Latonia dimenticata* was a large frog (potentially reaching 15 cm SVL, maybe more), which inhabited the marshy environment of the Pietrafitta Pleistocene swamp possibly feeding on molluscs and other hard invertebrates.

Recognition of evolutionary trends in *Latonia* is hindered by a limited understanding of the phylogenetic relationships within the genus. Our first attempt at a phylogenetic analysis performed with modern computational tools offers some interesting inferences, but it also opens new questions. According to our analysis, two different major *Latonia* clades may have existed in Europe since the early history of the genus, both leaving a single last representative each in the Pleistocene. *Latonia dimenticata* would be part of the least known of these two clades, which would only include *L. caucasica* from the Late Miocene of northern Caucasus in addition to the Italian species. The other clade, on the other hand, would include most of the other extinct species of *Latonia* currently known, and it would be present in the fossil record since the Oligocene. Its last representative is the Middle Pleistocene *Latonia* from Esztramos 6, in Hungary, which is also the youngest occurrence of the genus in Europe. The extant *L. nigriventer* would not be part of either of these two clades, but it would represent its own clade, diverging before the split of the two European ones. However, this may also result from the very peculiar (unsculptured) morphology of *L. nigriventer*, which might be a secondary evolution under paedomorphic conditions.

By observing the extended fossil record of the genus in Eurasia, *Latonia* with strongly developed cranial exostosis are common throughout the first part of the Miocene, in particular during the

hyperthermal phase named Miocene Climatic Optimum. Later, and especially starting from the Late Miocene, remains of *Latonia* are characterised by a reduced extension and less pustular nature of the cranial exostosis, a trend that is clearly exemplified in Pleistocene occurrences such as *L. dimenticata* sp. nov. (with its narrow facies dorsalis missing the tectum supraorbitale). This change in the morphology and development of the exostosis can be correlated with environmental changes, with the earliest members of *Latonia* having possibly evolved more sculptured crania to face drought in the warm Oligocene or at the Oligocene/Miocene transition and younger members reducing the cover in a progressively cooling interval after the Middle Miocene and through the Quaternary glacial cycles. Ultimately, rapid changes in the last glacial phases and the impact of these on the water bodies where *Latonia* would have spent its larval stages, may have prompted a different response in *L. nigriventer*, with a shortening of larval development leading to the paedomorphic morphology of the extant species.

This reconstruction provides us with a testable hypothesis on the main evolutionary trends characterizing the past and recent history of *Latonia*, which could undergo future scrutiny with the discovery of new fossils and the development of more detailed morphological and phylogenetic studies on the genus. Particular focus should be given to the search for *Latonia* frontoparietals dating back to the late Palaeogene, which is the time when the genus appeared and for which we have no real information on the presence and development of the exostosis on the skull roof, as well as for new fossils from western Asia and the Middle East in particular, to shed light on the early evolution of the lineage leading to the extant *L. nigriventer*. Additionally, an improvement in the understanding of the intrageneric phylogenetic relationships is also needed: apart for indicating a long ghost lineage in the Levant, the topology we recovered in our preliminary analysis points to an early-branching clade of completely unsculptured *Latonia*, and potentially even complete absence of exostosis as the plesiomorphic state for the whole genus, both things which are currently not supported by the fossil record (there are no smooth frontoparietals referred to *Latonia* in pre-Quaternary times and outside from the distributional area of the extant species). An expanded

phylogenetic matrix, with more characters and taxa, together with a renewed study of the osteological variation within *Latonia* and new fossils, will help resolve this conundrum.

Acknowledgements

L.S. is supported by a Humboldt Research Fellowship provided by the Alexandervon Humboldt Foundation. A.V. acknowledges financial support by the Secretaria d'Universitats i Recerca of the Departament de Recerca i Universitats, Generalitat de Catalunya, through a Beatriu de Pinós postdoctoral grant (2021 BP 00038), and the Agencia Estatal de Investigación of the Spanish Ministerio de Ciencia e Innovación (MCIN/AEI/10.13039/501100011033/), through the R+D+I project PID2020-117289GB-I00. Z.R. was supported by the research plan of the Institute of Geology of the Czech Academy of Sciences (RVO67985831). This project was also funded by the CERCA Programme/Generalitat de Catalunya. We would like to thank the following colleagues for help and discussions during the development of this study: Rebecca Biton (Be'er Sheva) and Renaud Boistel (Paris) for sharing information on *L. nigriventer*; Tassos Kotsakis, Chiara Angelone (both Roma), and Sergio Gentili (Perugia) for discussions on the *Latonia* fossils from Pietrafitta; Marco Pavia (Torino) for providing literature; as well as Loredana Macaluso and Jules Walter (both Torino) for help with the scorings and the phylogenetic analysis. We sincerely thank Paola Romi (SABAP_UMB) for having made the paleontological material of Pietrafitta available (and for the great enthusiasm on fossil frogs!), Tiziana Caponi (Direzione Regionale Musei Umbria), director of the Museo Paleontologico "Luigi Boldrini" in Pietrafitta, and the whole museum staff. We thank the Editor-in-Chief, Zerina Johanson, for handling our contribution, as well as the associate editor and the two reviewers, Paula Muzzopappa and Alfred Lemierre, who helped improving our article with their kind comments and suggestions on a previous version. We are deeply indebted to the staff of MorphoSource and of all the institutions and people that uploaded CT scans of the specimens used

to prepare the phylogenetic matrix, whose work was pivotal for the completion of this work. We thank the Willi Hennig Society for making TNT freely available. This is publication number XXX of the Museo di Geologia e Paleontologia collections at the Università degli Studi di Torino.

Disclosure statement

The authors report there are no competing interests to declare.

Data availability statement

Phylogenetic data for this study are available in MorphoBank (O'Leary & Kaufman, 2012) (http://morphobank.org/permalink/?P5094) **[review access, not to be shared without express permission from the authors: log in as P5094; password LatoniaPietrafitta]**

Supplemental material

Supplemental Material Table 1. Complete list of the *Latonia dimenticata* sp. nov. remains housed in the Museo Paleontologico "Luigi Boldrini" in Pietrafitta.

Supplemental Material File 1. Results of the fourth and fifth iterations of the performed phylogenetic analysis and apomorphy list for *Latonia* and its subclades.

References

Ambrosetti, P., Argenti, P., Basilici, G., Gentili, S., & Ikome, F. E. (1992). The pleistocenic fossil vertebrata of the Pietrafitta basin (Umbria, Italy): preliminary taphonomic analyses. Taphonomy: processes and products. *European Paleontological Association Workshop, Strasbourg*, *Abstract volume*, 20 –21.

Ambrosetti, P., Basilici, G., Capasso Barbato, L., Carboni, M. G., Di Stefano, G., Esu, D., Gliozzi, E., Petronio, C., Sardella, R., & Squazzini, E. (1995). Il Pleistocene inferiore nel ramo Sud-Occidentale del Bacino Tiberino (Umbria): aspetti litostratigrafici e biostratigrafici. *Il Quaternario*, *8*, 19–36.

Ambrosetti, P., Cattuto, C., & Gregori, L. (1989). Geomorfologia e neotettonica nel bacino di Tavernelle/Pietrafitta (Umbria). *Il Quaternario*, *2*, 57–4.

Ambrosetti, P., Faraone, A., & Gregori, L. (1987). Pietrafitta: un museo di paleontologia in Umbria. *Museologia Scientifica, 4,* 99–118.

Anderson, D. E., Goudie, A. S., & Parker, A. G. (2007). *Global environments through the Quaternary.* Oxford University Press.

Bailon, S. (1999). Différenciation ostéologique des anoures (Amphibia, Anura) de France. In J. Desse & N. Desse-Berset (Eds), *Fiches d'ostéologie animale pour l'Archéologie, Série C: Varia, 1* (pp. 1–41). APDCA.

Biton, R., Bailon, S., Birkenfeld, M., Bridault, A., Khalaily, H., Valla, F. R., & Rabinovich, R. (2021). The anurans and squamates assemblage from Final Natufian Eynan (Ain Mallaha, Israel) with an emphasis on snake-human interactions. *PLoS ONE*, *16*, e0247283.

Biton, R., Bailon, S., Goren-Inbar, N., Sharon, G., & Rabinovich, R. (2019). Pleistocene amphibians and squamates from the Upper Jordan Rift Valley, Gesher Benot Ya'aqov and Nahal Mahanayeem Outlet (MIS 20–18 and MIS 4/3). *Quaternary Research*, *91*, 345–366.

Biton, R., Boistel, R., Rabinovich, R., Gafny, S., Brumfeld, V., & Bailon, S. (2016). Osteological observations on the alytid anura *Latonia nigriventer* with comments on functional morphology, biogeography, and evolutionary history. *Journal of Morphology*, *277*, 1131–1145.

Biton, R., Geffen, E., Vences, M., Cohen, O., Bailon, S., Rabinovich, R., Malka, Y., Oron, T., Boistel, R., Brumfeld, V., & Gafny, S. (2013). The rediscovered Hula painted frog is a living fossil. *Nature Communications*, *4*, 1959.

Blackburn, D. C., Boyer D.M., Gray, J. A., Winchester, J., Bates, J. M., Baumgart, S. L., Braker, E., Coldren, D., Conway, K. W., Davis Rabosky, A., de la Sancha, N., Dillman, C. B., Dunnum, J. L., Early, C. M., Frable, B. W., Gage, M. W., Hanken, J., Maisano, J. A., Marks, B. D., Maslenikov, K. P., McCormack, J. E., Nagesan, R. S., Pandelis, G. G., Prestridge, H. L., Rabosky, D. L., Randall, Z. S., Robbins, M. B., Scheinberg, L. A., Spencer, C. L., Summers, A. P., Tapanila, L., Thompson, C. W., Tornabene, L., Watkins-Colwell, G. J., Welton, L. J., the oVert Project Team, & Stanley, E. L. (2024). Increasing the impact of vertebrate scientific collections through 3D-imaging: the openVertebrate (oVert) Thematic Collections Network. *BioScience, 74*, 169–186.

Bolkay, J. (1913), Additions to the fossil herpetology of Hungary from the Pannonian and Praeglacial periods. *Mitteilungen aus dem Jahrbuche der königlich ungarischen Geologischen Reichsanstalt*, *21*, 217–230.

Bolkay, J. (1919). Osnove uporedne osteologie anurskih batrahija. *Glasnik zemaljskog muzeja y Bosni i Hercegovini, 31*, 277–356.

Cherin, M., Bizzarri, R., Buratti, N., Caponi, T., Grossi, F., Kotsakis, T., Pandolfi, L., Pazzaglia, F., & Barchi, M. R. (2012). Multidisciplinary study of a new Quaternary mammal-bearing site from

Ellera di Corciano (central Umbria, Italy): preliminary data. *Rendiconti Online della Società Geologica Italiana*, *21*, 1075–1077.

Cherin, M., Iurino, D. A., Zanatta, M., Fernandez, V., Paciaroni, A., Petrillo, C., Rettori, R., & Sardella, R. (2018). Synchrotron radiation reveals the identity of the large felid from Monte Argentario (Early Pleistocene, Italy). *Scientific Reports*, *8*, 1–10.

Chkhikvadze, V. M. (1981). Review of evidence on fossil remains of amphibians and reptiles from the Neogene deposits of northern Black Sea coastal area. In L. S. Darevsky (Ed.), Fifth Herpetological Conference. The Problems of Herpetology (151–152). Nauka.

Conti, M. A., & Esu, D. (1981). Considerazioni sul significato paleoclimatico e geodinamico di una serie lacustre pleistocenica inferiore presso Tavernelle (Perugia, Umbria). *Geografia Fisica e Dinamica Quaternaria*, *4*, 3–10.

Conti, M. A., & Girotti, O. (1977). Il Villafranchiano nel "Lago Tiberino", ramo sud-occidentale: schema stratigrafico e tettonico. *Geologica Romana*, *16*, 67–80.

Dansgaard, W., White, J., & Johnsen, S. (1989). The abrupt termination of the Younger Dryas climate event. *Nature*, *339*, 532–534.

de Bonis, L., Crochet, J. Y., Rage, J.-C., Sigé, N., Sudre, J., & Vianey-Liaud, M. (1973). Nouvelles faunes de vertébrés oligocènes des Phosphorites du Quercy. *Bulletin du Muséum National d'Histoire Naturelle*, 174, 105–113.

Delfino, M. (2002). *Erpetofaune italiane del Neogene e del Quaternario* [Unpublished doctoral dissertation]. Università degli Studi di Modena e Reggio Emilia.

Dong, L., Roček, Z., Wang, Y., & Jones., M. E. H. (2013). Anurans from the Lower Cretaceous Jehol Group of Western Liaoning, China. *PLoS ONE*, *8*, e69723.

Dubois, A., Ohler, A., & Pyron, R. A. (2021). New concepts and methods for phylogenetic taxonomy and nomenclature in zoology, exemplified by a new ranked cladonomy of recent amphibians (Lissamphibia). *Megataxa*, *5*, 1–738.

Duellman, W. E., & Trueb, L. (1986). *Biology of Amphibians.* McGraw-Hill Company.

Duméril, A. M. C. (1805). *Zoologie analytique, ou méthode naturelle de classification des animaux, rendue plus facile à l'aide de tableaux synoptiques.* '1806'. Allais.

Evans, S. E., Groenke, J. R., Jones, M. E. H., Turner, A. H., & Krause, D. W. (2014). New material of *Beelzebufo*, a hyperossified frog (Amphibia: Anura) from the Late Cretaceous of Madagascar. *PLoS ONE*, *9*, e87236.

Féjérváry, G. J. (1917). Anoures fossiles des couches preglaciaires de Püspökfürdö en Hongrie. *Feldtani Közlöni*, *47*, 141–172.

Fey, B. (1988). Die Anurenfauna aus der Unterkreide von Uña (Ostspanien). *Berliner geowissenschaftliche Abhandlungen, Reihe A*, *Band 103*, 1–99.

Fitzinger, L. J. (1861). Eine Neue Batrachier-Gattung aus Neu-Seeland. *Verhandlungen der zoologisch-botanischen Vereins in Wiens*, *11*, 217–220.

Friant, M. (1944). Caractères anatomiques d'un batracien oligocène de la Limagne, le *Prodiscoglossus vertaizoni* nov. gen. nov. spec. *Comptes Rendus Hebdomadaires des Seances de l'Academie des Sciences*, *219*, 561–562.

Gardner, J. D., & Rage, J.-C. (2016). The fossil record of lissamphibians from Africa, Madagascar, and the Arabian Plate. *Palaeobiodiversity and Palaeoenvironments*, *96*, 169–220.

Gentili, S., Abbazzi, L., Masini, F., Ambrosetti, P., Argenti, P., & Torre, D. (1996). Voles from the Early Pleistocene of Pietrafitta (central Italy, Perugia). *Acta Zoologica Cracoviensia*, *3*, 185–199.

Gentili, S., Barili, A., & Ambrosetti, P. (2000). Un museo per i fossili di Pietrafitta. *Nuova Museologia*, *2*, 16–17.

Georgalis, G. L., Villa, A., Ivanov, M., & Delfino, M. (2024). New diverse amphibian and reptile assemblages from the late Neogene of northern Greece provide novel insights into the emergence of extant herpetofaunas of the southern Balkans. *Swiss Journal of Palaeontology, 143,* 34.

Gliozzi, E., Abbazzi, L., Argenti, P., Azzaroli, A., Caloi, L., Barbato, L. C., Di Stefano, G., Esu, D., Ficcarelli, G., Girotti, O., & Kotsakis, T. (1997). Biochronology of selected mammals, molluscs and ostracods from the Middle Pliocene to the Late Pleistocene in Italy. The state of the art. *Rivista Italiana di Paleontologia e Stratigrafia*, *103*, 369–388.

Goloboff, P. A., & Morales, M. E. (2023). TNT version 1.6, with a graphical interface for MacOS and Linux, including new routines in parallel. *Cladistics*, *39*, 144–153.

Gómez, R. O., & Turazzini, G. F. (2016). An overview of the ilium of anurans (Lissamphibia, Salientia), with a critical appraisal of the terminology and primary homology of main ilial features. *Journal of Vertebrate Paleontology*, *36*, e1030023.

Gray, J. E. (1825). A synopsis of the genera of Reptiles and Amphibia, with a description of some new species. *Annals of Philosophy*, *10*, 193–217.

Günther, A. (1858). On the systematic arrangement of the tailless batrachians and the structure of *Rhinophrynus dorsalis*. *Proceedings of the Zoological Society of London*, *26*, 339–352.

Hossini, S. (1993). A new species of *Latonia* (Anura, Discoglossidae) from the lower Miocene of France. *Amphibia-Reptilia*, *14*, 237–245.

Hossini, S. (2000). Un nouveau discoglossidé (Amphibia, Anura) dans le Miocène supérieur du gisement marocain « Oued Zra *». Comptes rendus de l'Académie des sciences. Série IIa - Sciences de la Terre et des Planètes*, *331*, 621–626.

Jánossy, D., & Kordos, L. (1977). Az Osztramos lelőhelyeinek faunisztikai és karsztmorfológiai áttekintése (1975). *Fragmenta Mineralogica et Paleontologica*, *8*, 39–72.

Ji, S., & Ji, Q. (1998). The first Mesozoic frog from China (Amphibia: Anura). *Chinese Geology*, *250*, 39–42.

Kovács, J., Moravcová, M., Újváry, G., & Pintér, A. G. (2012). Reconstructing the paleoenvironment of East Central Europe in the Late Pleistocene using the oxygen and carbon isotopic signal of tooth in large mammal remains. *Quaternary International*, *276/277*, 145–154.

Lartet, E. (1851). *Notice sur la Colline de Sansan, suivie d'une récapitulation des diverses espèces d'animaux vertébrés fossil, trouvés soit à Sansan, soit dans d'autres gisements du terrain tertiaire miocène dans le bassin Sous-Pyrenéen.* J. A. Portes.

Linnaeus, C. (1758). *Systema Naturae, per Regna Tria Naturae, secundum Classes, ordines, Genera, Species, cum Characteribus, differentiis, Synonymis, locis, tenth ed., Tomus I.* Laurentii Salvii.

Lona, F., & Bertoldi, R. (1972). La storia del Plio-Pleistocene Italiano in alcune sequenze vegetationali lacustri e marine. *Atti della Accademia Nazionale dei Lincei, Classe di Scienze Fisiche, Matematiche e Naturali, Memorie, Serie VIII*, *11*, 1–47.

Lynch, J. D. (1969). Taxonomic notes on Ecuadorian frogs (Leptodactylidae: *Eleutherodactylus*). *Herpetologica*, *25*, 262–274.

Martinetto, E., Bertini, A., Basilici, G., Baldanza, A., Bizzarri, R., Cherin, M., Gentili, S., & Pontini, M. R. (2014). The plant record of the Dunarobba and Pietrafitta sites in the Plio-Pleistocene palaeoenvironmental context of Central Italy. *Alpine and Mediterranean Quaternary*, *27*, 29–72.

Martinetto, E., Momohara, A., Bizzarri, R., Baldanza, A., Delfino, M., Esu, D., & Sardella, R. (2017). Late persistence and deterministic extinction of "humid thermophilous plant taxa of East

Asian affinity" (HUTEA) in southern Europe. *Palaeogeography, Palaeoclimatology, Palaeoecology*, *467*, 211–231.

Mendelssohn, H. & Steinitz, H. (1943). A new frog from Palestine. *Copeia*, *4*, 231–233.

Neuwied, M. A. P. (1824). Verzeichnis der Amphibien welche in zweiten Bande der Naturgeschichte Brasiliens von Prinz Max von Neuwied werden beschreiben Werden. *Isis von Oken*, *14*, 661–673.

O'leary, M. A., & Kaufman, S. G. (2012). *MorphoBank 3.0: web application for morphological phylogenetics and taxonomy.* http://www.morphobank.org

Oken, L. von (1816). *Lehrbuch der Naturgeschichte. Dritter Theil, Zoologie. Zweite Abtheilung, Fleischthiere.* Schmid.

Otth, A. (1837). Beschreibung einer neuen europäischen Froschgattung, *Discoglossus*. *Neue Denkschriften der Allgemeinen Schweizerischen Gesellschaft für die Gesammten Naturwissenschaften*, *1*, 1–8.

Paluh, D. J., Stanley, E. L., & Blackburn, D. C. (2020). Evolution of hyperossification expands skull diversity in frogs. *PNAS*, *117*, 8554–8562.

Pazzaglia, F., Barchi, M. R., Buratti, N., Cherin, M., Pandolfi, L., & Ricci, M. (2013). Pleistocene calcareous tufa from the Ellera basin (Umbria, central Italy) as a key for an integrated paleoenvironmental and tectonic reconstruction. *Quaternary International*, *292*, 59–70.

Perl, R. G. B., Gafny, S., Malka, Y., Renan, S., Woodhams, D. C., Rollins-Smith, L., Pask, J. D., Bletz, M. C., Geffen, E., & Vences, M. (2017). Natural history and conservation of the rediscovered Hula painted frog, *Latonia nigriventer*. *Contributions to Zoology*, *86*,11–37.

Púgener, L. A., & Maglia, A. M. (1997). Osteology and skeletal development of *Discoglossus sardus* (Anura: Discoglossidae). *Journal of Morphology, 233*, 267–286.

Rage, J.-C. (1984). La “Grande Coupure” Éocène/Oligocène et les herpétofaunes (Amphibiens et Reptiles): problèms du synchronisme des événements paléobiogéographiques. *Bulletin de la Société géologique de France*, *26*,1251–1257.

Rage, J.-C. (2016). Frogs (Amphibia, Anura) from the Eocene and Oligocene of the Phosphorites du Quercy (France). An overview. *Fossil Imprint*, *72*, 53–66.

Rage, J.-C., & Hossini, S. (2000). Les amphibiens du Miocène moyen de Sansan. *Mémoires du Muséum national d'Histoire naturelle*, *183*, 177–217.

Rage, J.-C., & Roček, Z. (2003). Evolution of anuran assemblages in the Tertiary and Quaternary of Europe, in the context of palaeoclimate and palaeogeography. *Amphibia-Reptilia*. *24*, 133–167.

Ricciardi, E. (1961). Analisi pollinologica dei sedimenti lacustri lignitiferi di Pietrafitta (Perugia, Italia). *Pollen et Spores*, *3*, 325–328.

Roček, Z. (1994). Taxonomy and distribution of tertiary discoglossids (Anura) of the genus *Latonia* v. Meyer, 1843. *Geobios*, *27*, 717–751.

Roček, Z. (2013). Mesozoic and Tertiary Anura of Laurasia. *Palaeobiodiversity and Palaeoenvironments*, *93*, 397–439.

Roček, Z. (2019). A contribution to the herpetofauna from the late Miocene of Gritsev (Ukraine). *Comptes Rendus Palevol*, *18*, 817–847.

Roček, Z., Baleeva, N., Vazeille, A., Bravin, A., van Dijk, E., Nemoz, C., Přikryl, T., Smirina, E. M., Boistel, R., & Claessens, L. (2016). Contribution to the head anatomy of the basal frog *Barbourula busuangensis* and the evolution of the Anura. *Russian Journal of Herpetology*, *23*, 163–194.

Sanchiz, B. (1998a). *Handbuch der Paläoherpetologie. 4 - Salientia.* Friedrich Pfeil.

Sanchiz, B. (1998b). Vertebrates from the Early Miocene lignite deposits of the opencast mine Oberdorf (Western Styrian Basin, Austria): 2. Amphibia. *Annalen des Naturhistorischen Museums in Wien*, *99A*, 13–29.

Seibert, E. A., Lillywhite, H. B., & Wassersug, R. J. (1974). Cranial co-ossification in frogs: relationships to evaporative water loss. *Physiological Zoology*, *47*, 261–265.

Sorbelli, L., Cherin, M., Kostopoulos, D. S., Sardella, R., Mecozzi, B., Plotnikov, V., Prat-Vericat, M., Azzarà, B., Bartolini-Lucenti, S., & Madurell-Malapeira, J. (2023). Earliest bison dispersal in Western Palearctic: Insights from the *Eobison* record from Pietrafitta (Early Pleistocene, central Italy). *Quaternary Science Reviews*, *301*, 107923.

Sorbelli, L., Villa, A., Gentili, S., Cherin, M., Carnevale, G., Tschopp, E., & Delfino, M. (2021). The Early Pleistocene ectothermic vertebrates of Pietrafitta (Italy) and the last Western European occurrence of *Latonia* Meyer, 1843. *Comptes Rendus Palevol*, *20*, 555–583.

Špinar, Z. V. (1976). Endolymphatic sacs and dorsal endocranial pattern: Their significance for systematics and phylogeny of frogs. *Vestník Ústredního Ústavu Geologického*, *51*, 285–290.

Špinar, Z. (1978). *Latonia kolebabi* Špinar, 1976 (Amphibia) and remarks on the "genus *Miopelobates*". In V. Pokorný (Ed.), *Paleontologická konference 1977* (pp. 289–303). Charles University.

Steinthorsdottir, M., Coxall, H. K., De Boer, A. M., Huber, M.., Barbolini, N., Bradshaw, C. D., Burls, N. J., Feakins, S. J., Gasson, E., Henderiks, J., Holbourn, A. E., Kiel, S., Kohn, M. J., Knorr, G., Kürschner, W. M., Lear, C. H., Liebrand, D., Lunt, D. J., Mörs, T., Pearson, P. N., Pound, M. J., Stoll, H., & Strömberg, C. A. E. (2021). The Miocene: the future of the past. *Paleoceanography and Paleoclimatology*, *36*, e2020PA004037.

Stejneger, L. (1899). Description of a new genus and species of discoglossoid toad from North America. *Proceedings of the United States National Museum*, *21*, 899–901.

Stephenson, E. M. (1951). The anatomy of the head of the New Zealand frog, *Leiopelma*. *The Transactions of the Zoological Society of London*, *27*, 255–305.

Syromyatnikova, E., & Roček, Z. (2019). New *Latonia* (Amphibia: Alytidae) from the late Miocene of northern Caucasus (Russia). *Palaeobiodiversity and Palaeoenvironments*, *99*, 495–509.

Syromyatnikova, E., Georgalis, G. L., Mayda, S., Kaya, T., & Saraç, G. (2019). A new early Miocene herpetofauna from Kilçak, Turkey. *Russian Journal of Herpetology*, *26*, 205–224.

Syromyatnikova, E., Mayda, S., & Tesakov, A. (2022). Late Miocene amphibians and reptiles: new insight into the pre-Messinian herpetofaunas in Turkey. *Historical Biology*, *34*, 1964–1971.

Syromyatnikova, E., Roček, Z., & van de Velde, S. (2019). New discoveries in the frog *Latonia seyfriedi* (Anura: Alytidae) and their impact on taxonomy of the genus *Latonia*. *PalZ*, *93*, 669–677.

Syromyatnikova, E., Tesakov, A., Mayda, S., Kaya, T., & Saraç, G. (2019). Plio-Pleistocene amphibians and reptiles from central Turkey: new faunas and faunal records with comments on their biochronological position based on small mammals. *Fossil Imprints*, *75*, 343–358.

Szentesi, Z. (2019). *Latonia gigantea* (Lartet, 1851) remains and other herpetological observations from the middle Pleistocene Esztramos 6 locality (Aggtelek–Rudabánya Mountains, North Hungary). *Fragmenta Palaeontologica Hungarica*, *36*, 141–158.

Tatarinov, K. A. (1970). *Fauna of the Neogene vertebrates* [Unpublished abstract of doctorate dissertation]. University of Kiev.

Taylor, E. H., & Noble, G. K. (1924). A new genus of discoglossid frogs from the Philippine Islands. *American Museum Novitates*, *121*, 1–4.

Tschudi, J. J. (1838). *Classification der Batrachier, mit Berücksichtigung der fossilen Thiere dieser abteilung der Reptilien.* Petitpierre.

Vasilyan, D., Roček, Z., Ayvazyan, A., & Claessens, L. (2019). Fish, amphibian and reptilian faunas from latest Oligocene to middle Miocene localities from Central Turkey. *Palaeobiodiversity and Palaeoenvironments*, *99*, 723–757.

Vasilyan, D., Schneider, S., Bayraktutan, M. S., & Şen, Ş. (2014). Early Pleistocene freshwater communities and rodents from the Pasinler Basin (Erzurum Province, north-eastern Turkey). *Turkish Journal of Earth Sciences*, *23*, 293–307.

Venczel, M. (2001). Anuran and squamates from the lower Pliocene (MN 14) Osztramos 1 locality (Northern Hungary). *Fragmenta Palaeontologica Hungarica*, *19*, 79–90

Vergnaud-Grazzini, C. (1970). Les amphibiens fossils du gisement d'Arondelli. *Palaeontographia Italica*, *66*, 47–65.

Villa, A., Carnevale, G., Pavia, M., Rook, L., Sami, M., Szyndlar, Z., & Delfino, M. (2021). An overview of the late Miocene vertebrates from the fissure fillings of Monticino Quarry (Brisighella, Italy), with new data on non-mammalian taxa. *Rivista Italiana di Paleontologia e Stratigrafia, 127*, 297–354.

Villa, A., Delfino, M., Luján, À. H., Almécija, S., & Alba, D. M. (2019). First record of *Latonia gigantea* (Anura, Alytidae) from the Iberian Peninsula. *Historical Biology*, *31*, 371–382.

Villa, A., Macaluso, L., & Mörs, T. (2024). Miocene and Pliocene amphibians from Hambach (Germany): New evidence for a late Neogene refuge in northwestern Europe. *Palaeontologia Electronica*, *27*, a3.

Villalta, J. F. de (1954). Novedades paleomastológicas desde el último cursillo (1952). II Cursillo Internacional Paleontología, Museo de Sabadell, Sabadell.

von Meyer, H. (1843). Mittheilungen an Professor Bronn gerichtet. *Neues Jahrbuch für Mineralogie, Geognosie, Geologie und Petrefaktenkunde*, *1843*, 579–590.

Wagler, J. (1829). Descriptiones et icones Amphibiorum. *Isis von Oken*, *1829*, 68–70.

Wagler, J. (1830). *Natürliches System der Amphibien, mit vorangehender Classification der Säugthiere und Vogel. Ein Beitrag zur vergleichenden Zoologie.* J. G. Cotta.

Wang, Y., & Gao, K. (1999). Earliest Asian discoglossid frog from western Liaoning. *Chinese Science Bulletin*, *44*, 636–642.

Wuttke, M., Přikryl, T., Ratnikov, V. Yu., Dvořak, Z., & Roček, Z. (2012). Generic diversity and distributional dynamics of the Palaeobatrachidae (Amphibia: Anura). *Palaeobiodiversity and Palaeoenvironments*, *92*, 367–395.

You, Y., Huber, M., Müller, R. D., Poulsen, C. J., & Ribbe, J. (2009). Simulation of the Middle Miocene Climate Optimum. *Geophysical Research Letters*, *36*, L04702.

Zachos, J., Pagani, M., Sloan, L., Thomas, E., & Billups, K. (2001). Trends, rhythms and aberrations in global climate 65 Ma to present. *Science*, *292*, 686–693.

Figure captions

Figure 1. Location of the study area. A, The site of Pietrafitta (red star) lies within the Tavernelle-Pietrafitta Basin, between the wider Valdichiana Basin to the west and the Tiberino Basin to the east. B, Photographic view of one of the Pietrafitta quarry fronts. Interbedding of lignite and, secondarily, clay layers is visible. C, *Latonia dimenticata* sp. nov., paratype SABAP_UMB 24.4.1018 in the original plaster jacket photographed soon after discovery.

Figure 2. *Latonia dimenticata* sp. nov., cranial elements of the holotype SABAP_UMB 24.4.1019: A–D, right (A–B) and left (C–D) maxillae (SABAP_UMB 24.4.1019a) in medial (A, C) and lateral (B, D) views; E–F, right nasal (SABAP_UMB 24.4.1019b) in dorsal (E) and ventral (F) views; G–J, anterior (G, I) and posterior (H, J) portions of the frontoparietal (SABAP_UMB 24.4.1019c) in

dorsal (G–H) and ventral (I–J) views; K–M, left prooticooccipital (SABAP_UMB 24.4.1019d) in anterior (K), posterior (L), dorsal (M) and ventral (N) views. Scale bar equals 5 mm. Abbreviations: ClHy, Canal for the hyomandibular of the facial nerve; CoOc, condylus occipitalis; CrDe, crista dentalis; CrPi, crista parotica; FcPP, facies prootico–parietalis; H, horn; InFr, incrassation frontoparietalis; LaHo, lamina horizontalis; MaOc, margo occipitalis; MeCr, median crest; PqCA, palatoquadrate contact area; PoDe, posterior depression; PrPo, processus posterior; PrZy, processus zygomaticomaxillaris; PrPt, processus pterygoideus; PaCt, pars contacta; PmDSP, prominentia ducti semicircularis posterioris; PrPc, processus paraoccipitalis; PrPCL, processus prooticus caudalis; PrPRB, processus prooticus rostralis brevis; SuVJ: sulcus venae jugularis.

Figure 3. *Latonia dimenticata* sp. nov., angulars of the holotype SABAP_UMB 24.4.1019: A–D, left angular (SABAP_UMB 24.4.1019e) in dorsal (A), ventral (B), lateral (C) and medial (D) views; E–H, right angular (SABAP_UMB 24.4.1019f) in dorsal (E), ventral (F), lateral (G) and medial (H) views. Scale bar equals 5 mm. Abbreviations: ExSp, extremitas spatulata; PrCn, processus coronoideus; PrPn, processus paracoronoideus; SuMk; sulcus pro cartilago Meckeli.

Figure 4. *Latonia dimenticata* sp. nov., axial elements of the holotype SABAP_UMB 24.4.1019: A–F, atlas (SABAP_UMB 24.4.1019g) in dorsal (A), ventral (B), right lateral (C), anterior (D), posterior (E) and left lateral (F) views; G–K, presacral vertebra (SABAP_UMB 24.4.1019h) in ventral (G), dorsal (H), right lateral (I), anterior (J), posterior (K) and left lateral (L) views; M) urostyle (SABAP_UMB 24.4.1019j) in dorsal view. Scale bars equal 5 mm. Abbreviations: CaNe, carina neuralis; CrVe, crista ventralis; Poz, postzygapophysis; PrSn, processus spinosus; Prz, prezygapophysis; TrPr, transverse process.

Figure 5. *Latonia dimenticata* sp. nov., pectoral and forelimb elements of the holotype SABAP_UMB 24.4.1019: A–B, left coracoid (SABAP_UMB 24.4.1019l) in dorsal (A) and anterior (B) views; C–F, right (C–D) and left (E–F) scapulae (SABAP_UMB 24.4.1019m) in dorsal (C, F) and ventral (D–E) views; G–J, proximal (G–H) and distal (I–J) portions of left humerus

(SABAP_UMB 24.4.1019n) in ventral (G, I) and dorsal (H, J) views; K–M, right radioulna (SABAP_UMB 24.4.1019o) in distal (K), medial (L) and lateral (M) views. Scale bar equals 5 mm. Abbreviations: CmAn, collum antebrachii; CpHu, caput humeri; EpRa; epicondylus radialis; EpUl, epicondylus ulnaris; ImGl, intumescentia glenoidalis; Ol, olecranon; PaEp, pars epicoracoidealis; PaGl pars glenoidalis; PaSc, pars suprascapularis; Ra, radius; Ul, ulna; and as in Fig. 4.

Figure 6. *Latonia dimenticata* sp. nov., pelvic and hind limb elements of the holotype SABAP_UMB 24.4.1019: A–B, left ilial shaft (part of SABAP_UMB 24.4.1019r) in lateral (A) and medial (B) views; C–E, right ilial body (SABAP_UMB 24.4.1019q) in lateral (C), medial (D) and posterior (E) views; F–G, right femur (part of SABAP_UMB 24.4.1019s) in ventral (F) and posterior (G) views; H–K, right (H–I) and left (J–K) tibiofibulae (SABAP_UMB 24.4.1019t) in dorsal (H, K) and ventral (I–J) views; L, ?right tibiale (SABAP_UMB 24.4.1019u) in anterior view; M, ?right fibulare (SABAP_UMB 24.4.1019v) in anterior view; N–O, phalanx (part of SABAP_UMB 24.4.1019y) in ventral (N) and dorsal (O) views. Scale bar equals 5 mm. Abbreviations: AcFo, acetabular fossa; CrCu, crista cruris; CrFe, crista femoris; DoTu, dorsal tubercle; Fi, Fibula; FoTS, fossula tuberis superioris; PaAs, pars ascendens; PaDe, pars descendens; StFo, supraacetabular fossa; SuDi, sulcus distalis; SuPx, sulcus proximalis; Ti, Tibia.

Figure 7. *Latonia dimenticata* sp. nov., cranial elements of the paratype SABAP_UMB 24.4.1018: A–B, left premaxilla (SABAP_UMB 24.4.1018a) in posterior (A) and anterior (B) views; C–F, right (C–D) and left (E–F) maxillae (SABAP_UMB 24.4.1018b) in medial (C, E) and lateral (D, F) views; G–H, frontoparietal (SABAP_UMB 24.4.1018c) in ventral (G) and dorsal (H) views; I–L, right (I–J) and left (K–L) pterygoids (SABAP_UMB 24.4.1018d) in ventral (I, K) and dorsal (J, L) views. Scale bars equal 5 mm. Abbreviations: PaFa, pars facialis; PaPl, pars palatina; ReMs, recessus marsupiatus; RaMx, ramus maxillaris; SuPt, sulcus pterygoideus; VeFl, ventral flange; and as in Fig. 2.

Figure 8. *Latonia dimenticata* sp. nov., prooticooccipitals of the paratype SABAP_UMB 24.4.1018: A–D, right and, E–H, left prooticooccipitals (SABAP_UMB 24.4.1018f) in anterior (A, E), posterior (B, F), dorsal (C, G) and ventral (D, H) views. Scale bar equals 5 mm. Abbreviations as in Fig. 2.

Figure 9. *Latonia dimenticata* sp. nov., angulars of the paratype SABAP_UMB 24.4.1018: A–D, left and, E–H, right angulars (SABAP_UMB 24.4.1018g) in dorsal (A, E), ventral (B, F), lateral (C, G) and medial (D, H) views. Scale bar equals 5 mm. Abbreviations as in Fig. 3.

Figure 10. *Latonia dimenticata* sp. nov., axial elements of the paratype SABAP_UMB 24.4.1018: A, rib (part of SABAP_UMB 24.4.1018k) in either anterior or posterior view; B–E, urostyle (SABAP_UMB 24.4.1018m) in anterior (B), dorsal (C), ventral (D) and left lateral (E) views. Scale bar equals 5 mm. Abbreviations: ClCc, canalis coccygeus; FoCo, fossa condylodea; IvCl, intervertebral canal; UnPr, uncinate process; and as in Fig. 4.

Figure 11. *Latonia dimenticata* sp. nov., pectoral and forelimb elements of the paratype SABAP_UMB 24.4.1018: A–B, left coracoid (SABAP_UMB 24.4.1018n) in dorsal (A) and ventral (B) views; C–D, left scapula (SABAP_UMB 24.4.1018p) in ventral (C) and dorsal (D) views; E–H, left (E–F) and right (G–H) clavicles (SABAP_UMB 24.4.1018q) in ventral (E, H) and dorsal (F–G) views; I–L, left (I–J) and right (K–L) humeri (SABAP_UMB 24.4.1018r) in ventral (I, K) and dorsal (J, L) views; M) right radioulna (SABAP_UMB 24.4.1018t) in medial view. Scale bar equals 5 mm. Abbreviations: CrLa, crista lateralis; CrMe, crista medialis; FoCV, fossa cubitalis ventralis; PaAm, pars acromialis; SuCP, sulcus cartilagine praecoracoidealis; SiIg, sinus interglenoidalis; TeC tenuitas cranialis; and as in Fig. 5.

Figure 12. *Latonia dimenticata* sp. nov., pelvic and hind limb elements of the paratype SABAP_UMB 24.4.1018: A–E, left (A–B) and right (C–E) ilia (SABAP_UMB 24.4.1018u) in lateral (A, C), medial (B, D) and posterior (E) views; F, ischium (SABAP_UMB 24.4.1018v) in left lateral view; G, left femur (part of SABAP_UMB 24.4.1018w) in ventral view; H–K, right (H–I)

and left (J–K) tibiofibulae (SABAP_UMB 24.4.1018x) in dorsal (H, J) and ventral (I, K) views. Scale bar equals 5 mm. Abbreviations: DoCr, dorsal crest; IlGr, interiliac groove; and as in Fig.6.

Figure 13. *Latonia dimenticata* sp. nov., paratypes: A–D, right prooticooccipital (SABAP_UMB 24.4.1020) in anterior (A), posterior (B), dorsal (C) and ventral (D) views; E–F, left humerus (SABAP_UMB 24.4.1021) in ventral (E) and dorsal (F) views; G–J, ?right fibulare (G–H) and ?right tibiale (I–J) (SABAP_UMB 24.4.1022) in anterior (G, I) and posterior (H, J) views. Scale bar equals 5 mm. Abbreviations as in Figs. 2 and 5.

Figure 14. Results of the second and third iterations of the phylogenetic analysis: A, strict consensus of four most parsimonious trees resulting from the second iteration of the analysis; B, single most parsimonious tree resulting from the third iteration of the analysis.

Figure 15. Artistic reconstruction of *Latonia dimenticata* sp. nov.: A–C, osteological reconstruction of the skull in dorsal (A), right lateral (B) and ventral (C) views with preserved elements evidenced by numbers (1, praemaxilla; 2, maxilla; 3, nasal; 4, frontoparietal; 5, pterygoid; 6, prooticooccipital); D, in–life reconstruction. Drawings by Leonardo Sorbelli.

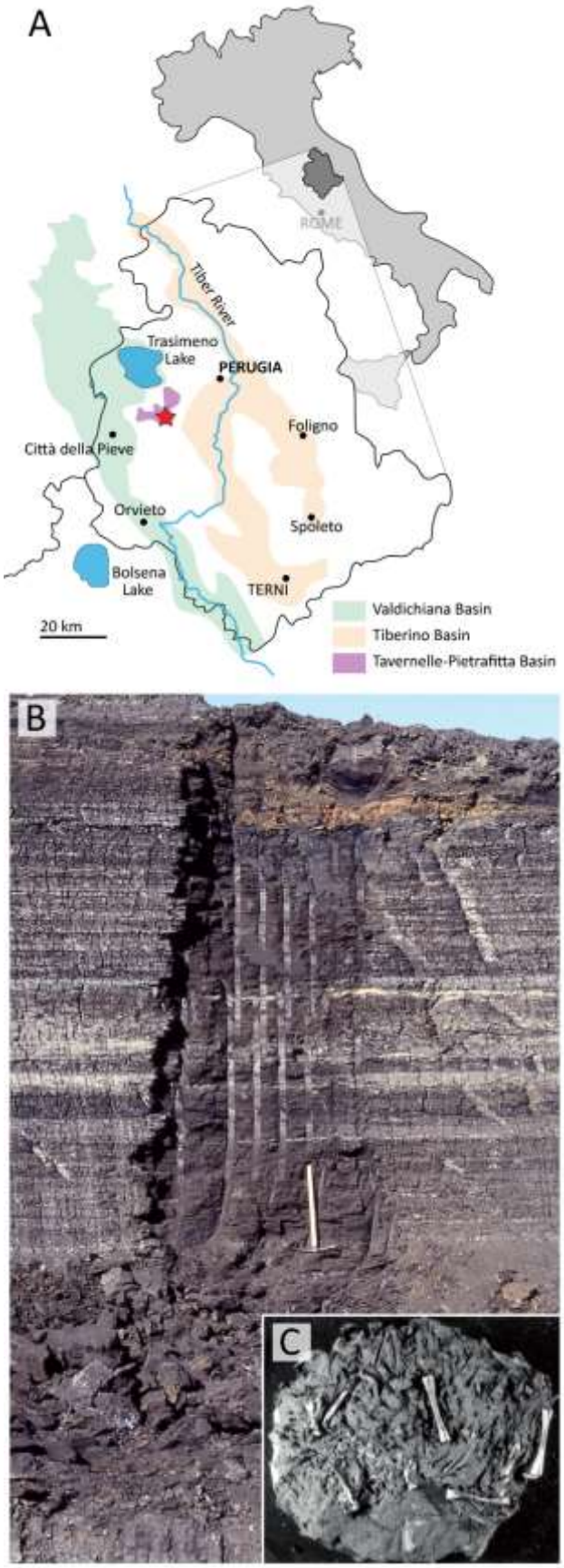

A
ROME
Tiber River
Trasimeno Lake
PERUGIA
Foligno
Città della Pieve
Orvieto
Spoleto
Bolsena Lake
TERNI
20 km
Valdichiana Basin
Tiberino Basin
Tavernelle-Pietrafitta Basin
B
C

Figure 1

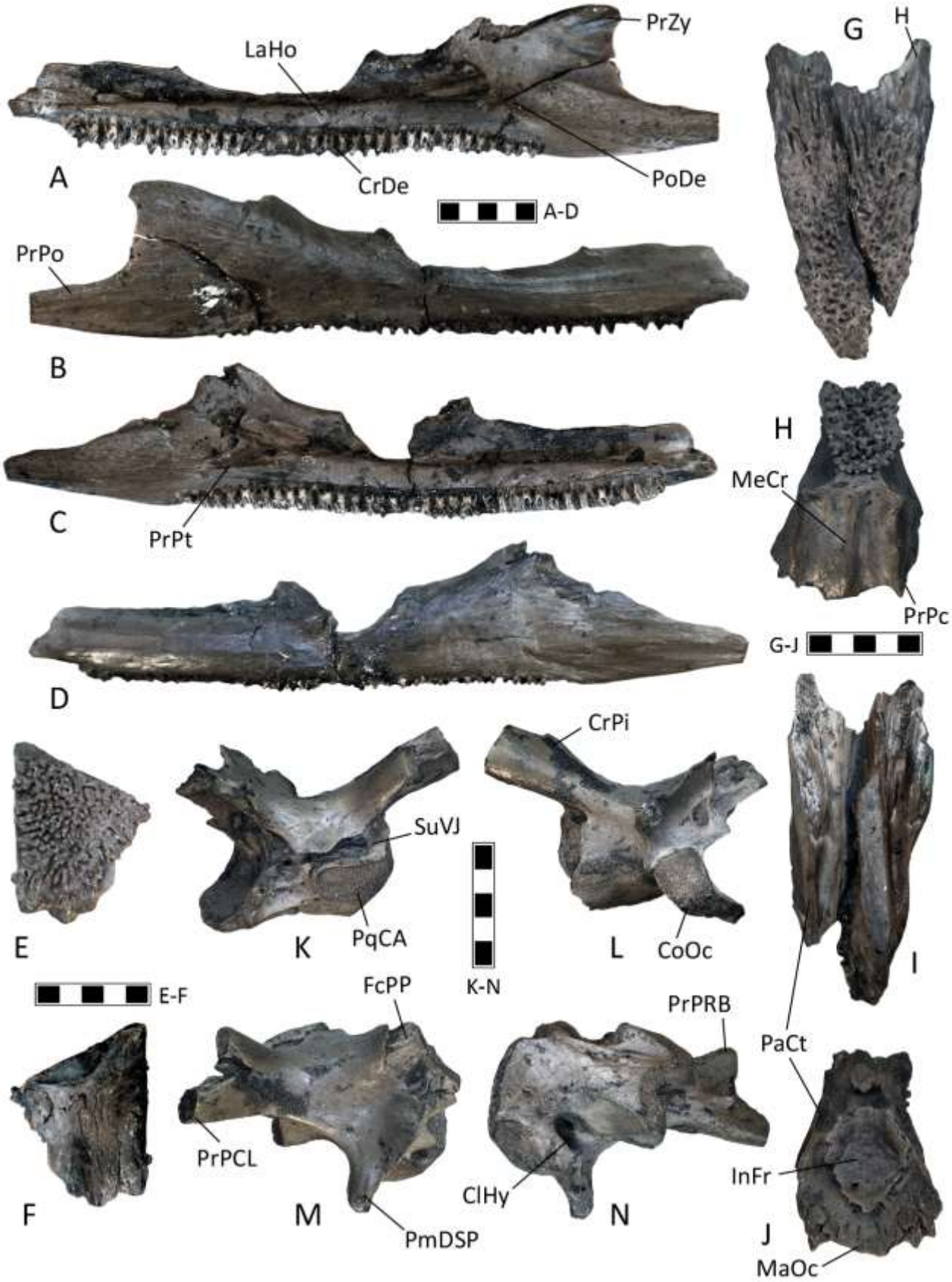

PrZy
LaHo
A
CrDe
PoDe
A-D
PrPo
B
C
PrPt
D
G
H
H
MeCr
PrPc
G-J
CrPi
SuVJ
E
K
PqCA
L
CoOc
I
K-N
E-F
FcPP
PrPRB
PaCt
F
PrPCL
M
ClHy
N
InFr
J
PmDSP
MaOc

Figure 2



Figure 3

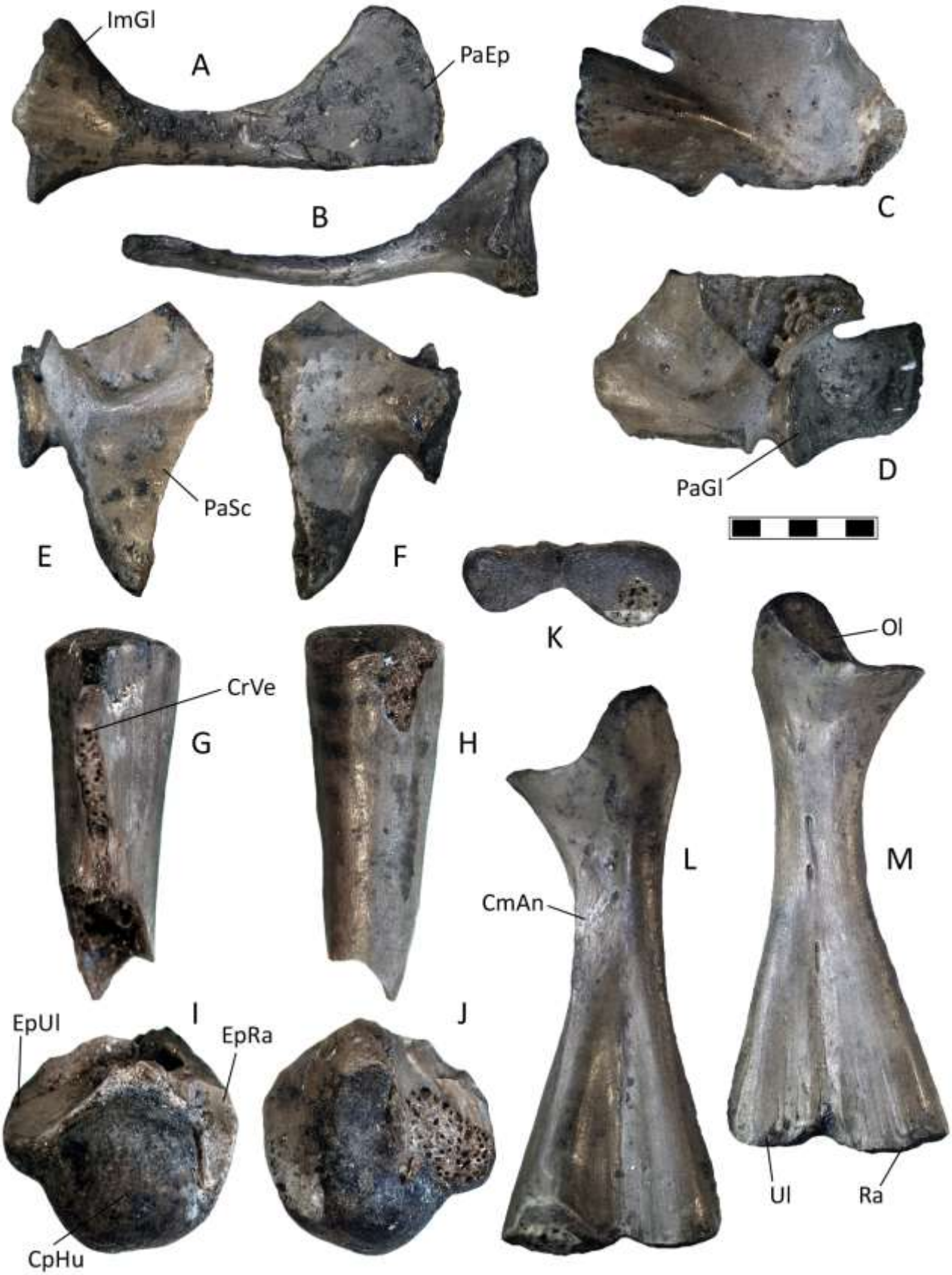

ImGl
A
PaEp
B
C
PaSc
E
F
PaGl
D
K
Ol
CrVe
G
H
L
M
CmAn
EpUl
EpRa
I
J
Ul
Ra
CpHu

Figure 4

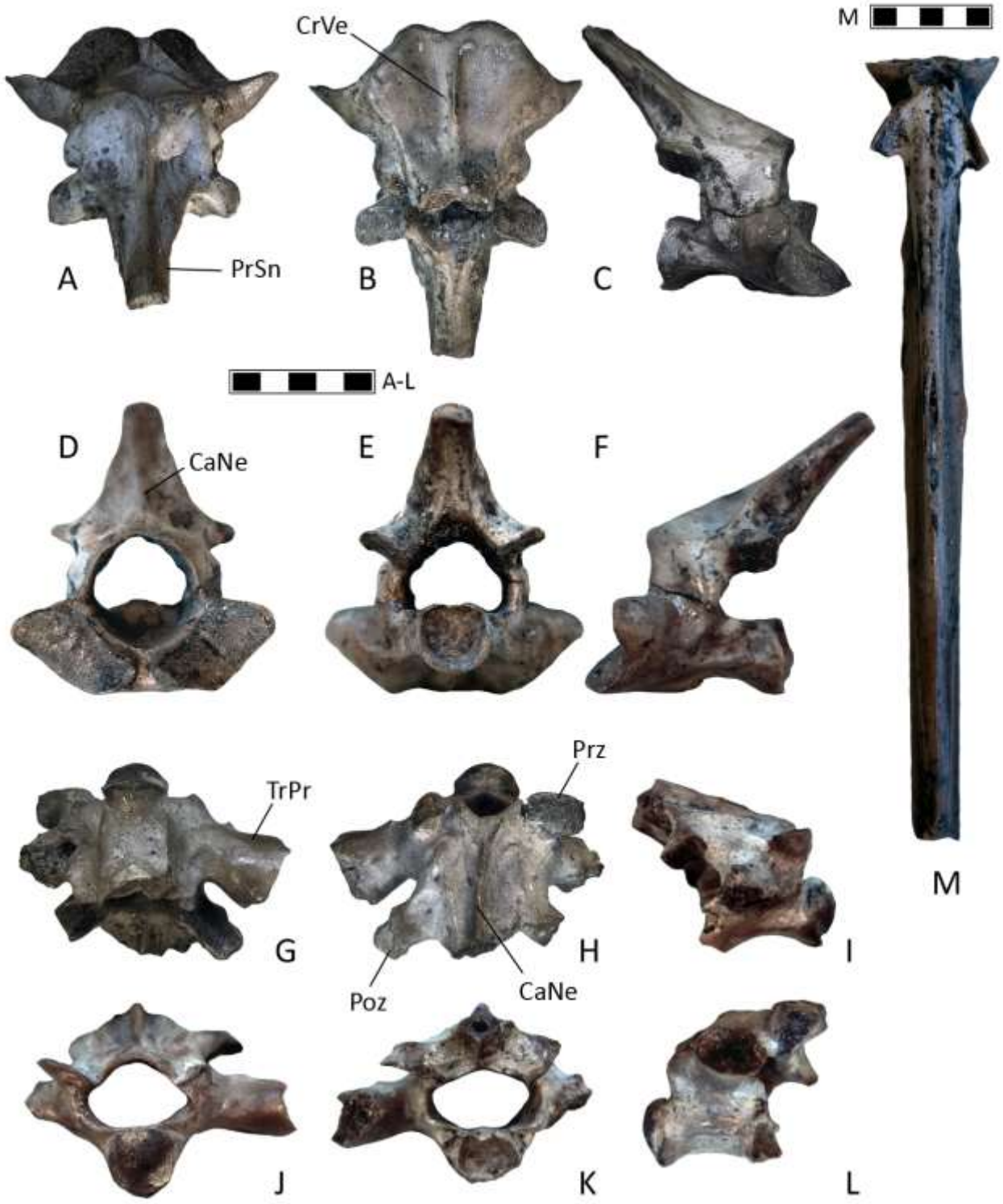


Figure 5

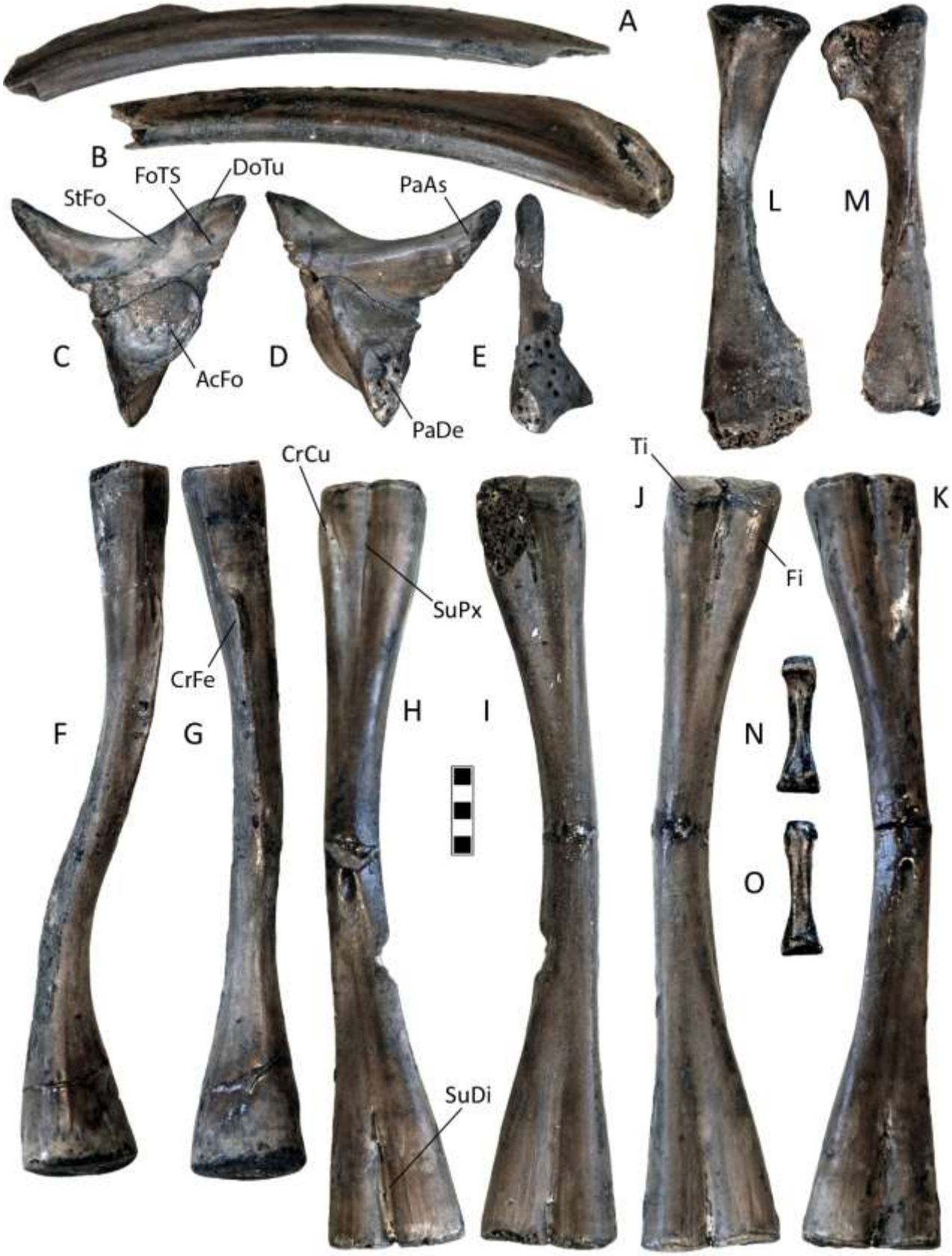

A
B
FoTS
DoTu
StFo
PaAs
C
AcFo
D
PaDe
E
L
M
CrCu
Ti
J
K
Fi
SuPx
CrFe
F
G
H
I
N
O
SuDi

Figure 6

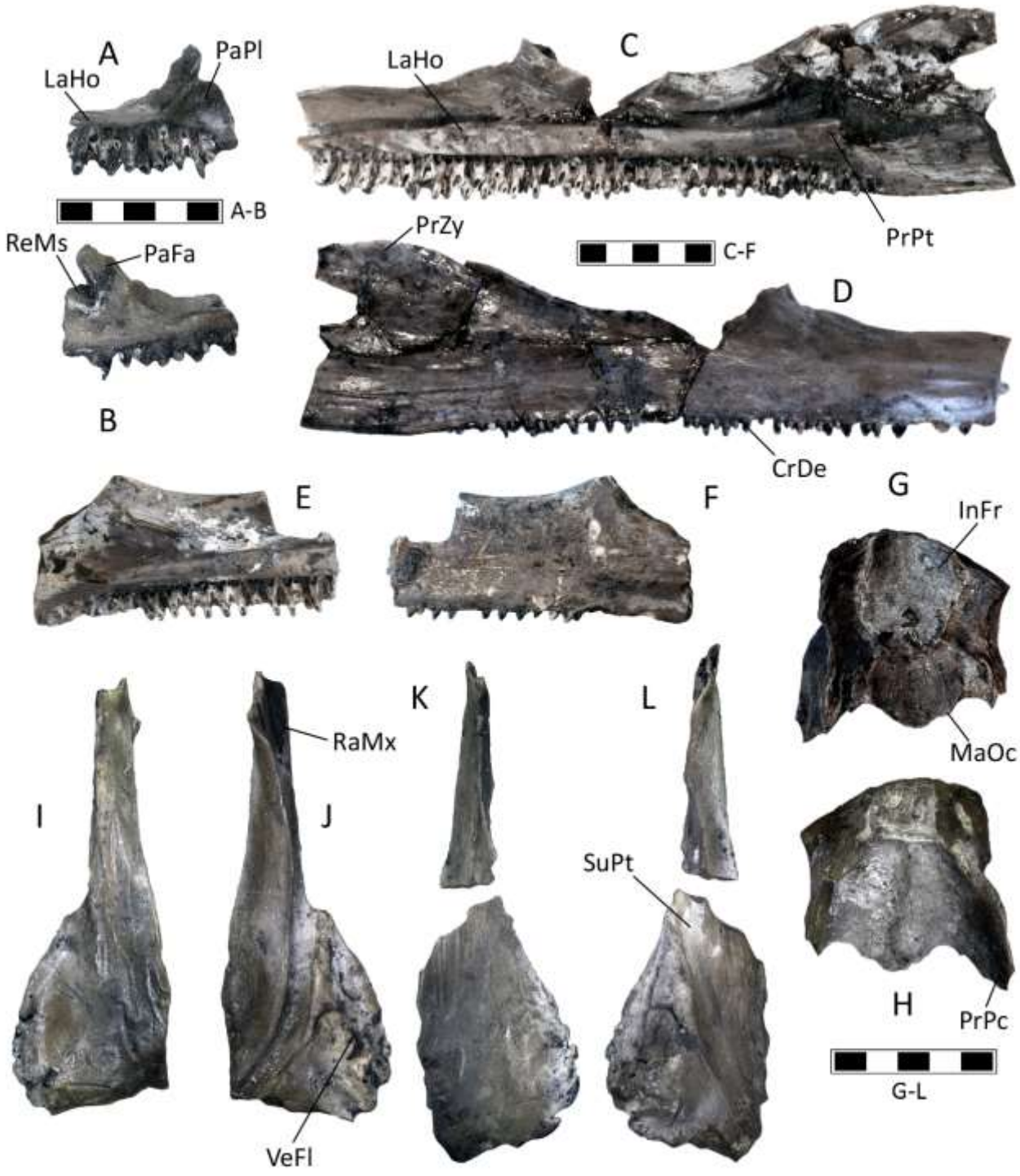

A
PaPl
LaHo
A-B
ReMs
PaFa
B
C
LaHo
PrZy
C-F
PrPt
D
CrDe
E
F
G
InFr
MaOc
I
RaMx
J
K
L
SuPt
H
PrPc
G-L
VeFl

Figure 7

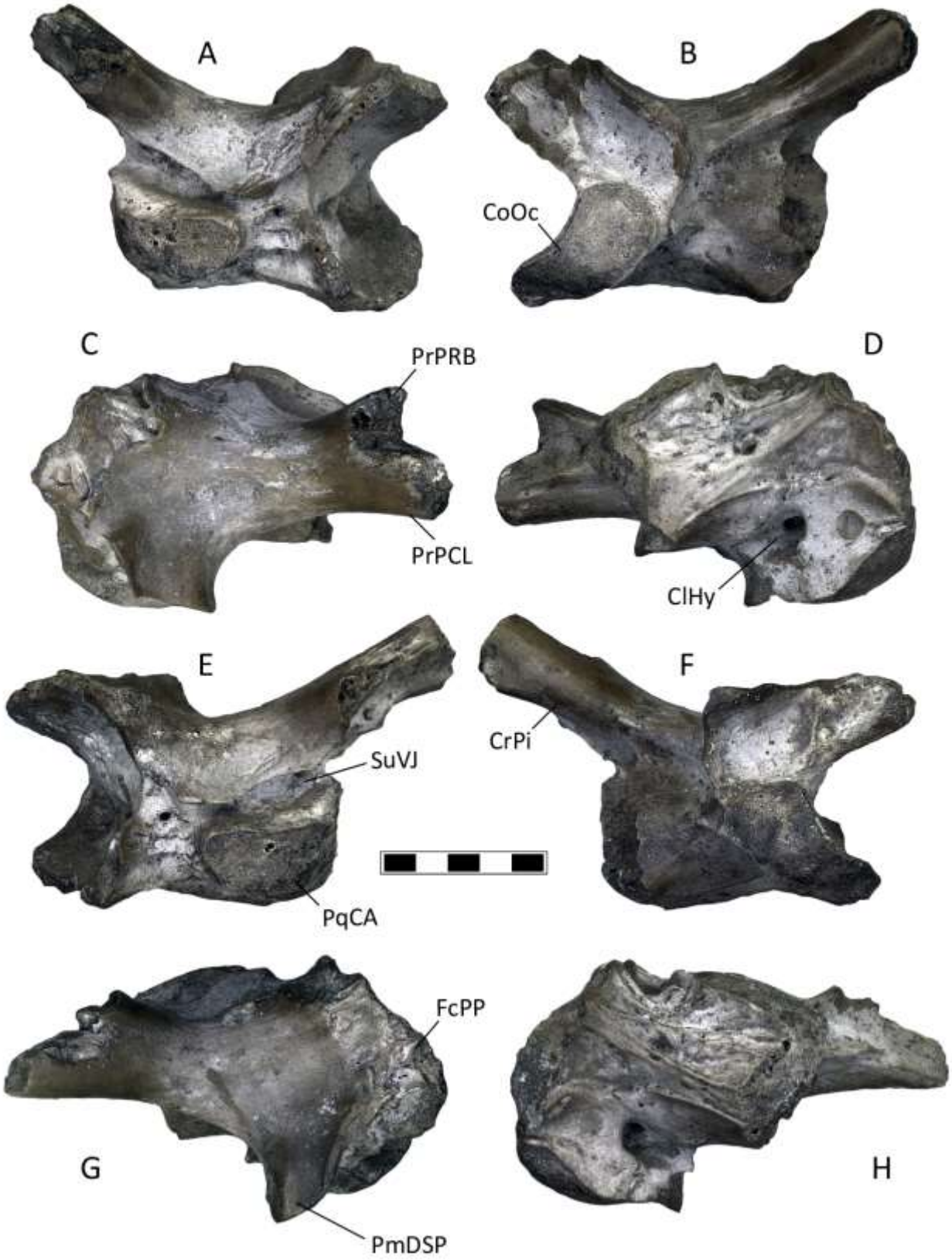


Figure 8



Figure 9

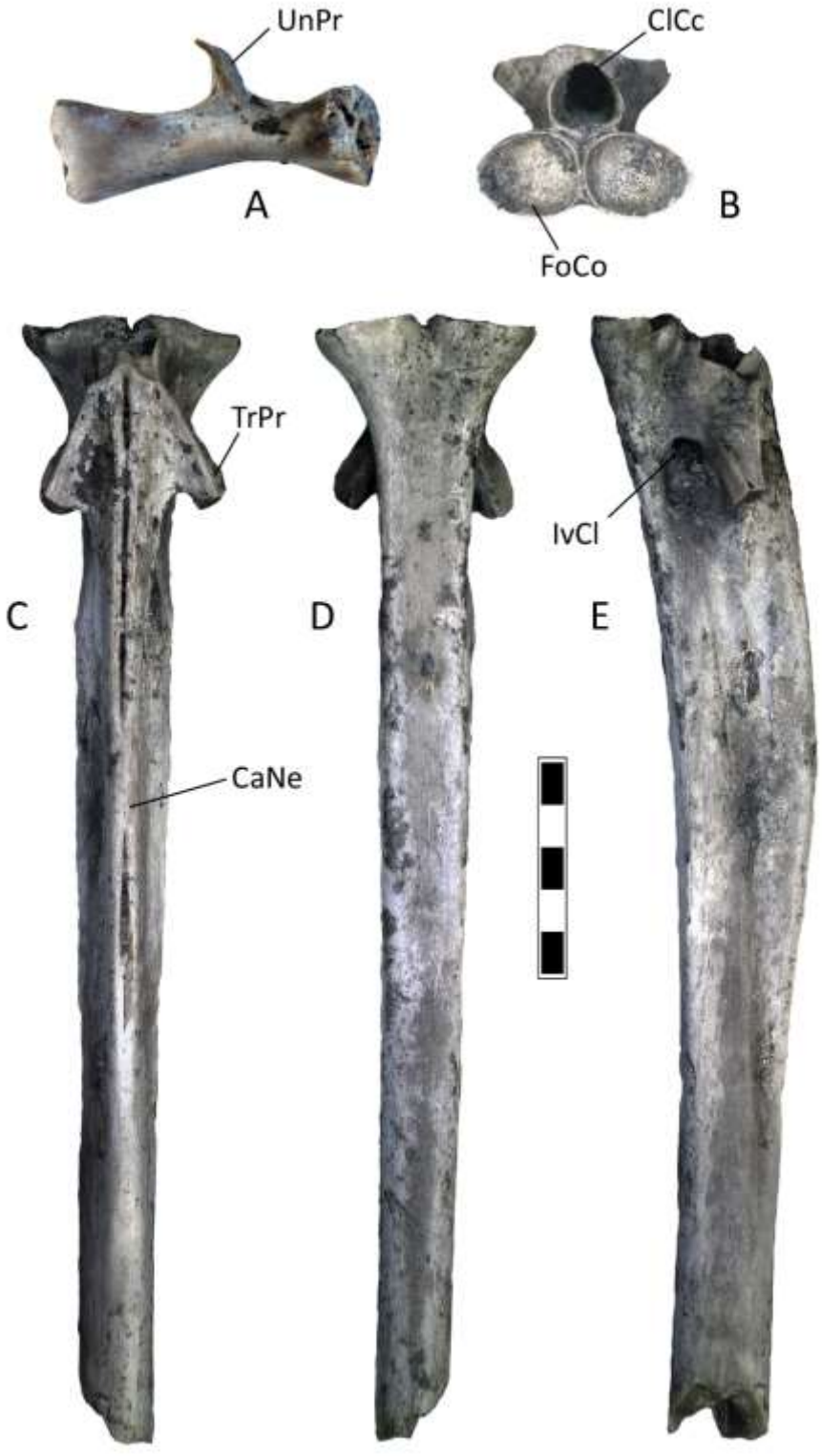


Figure 10

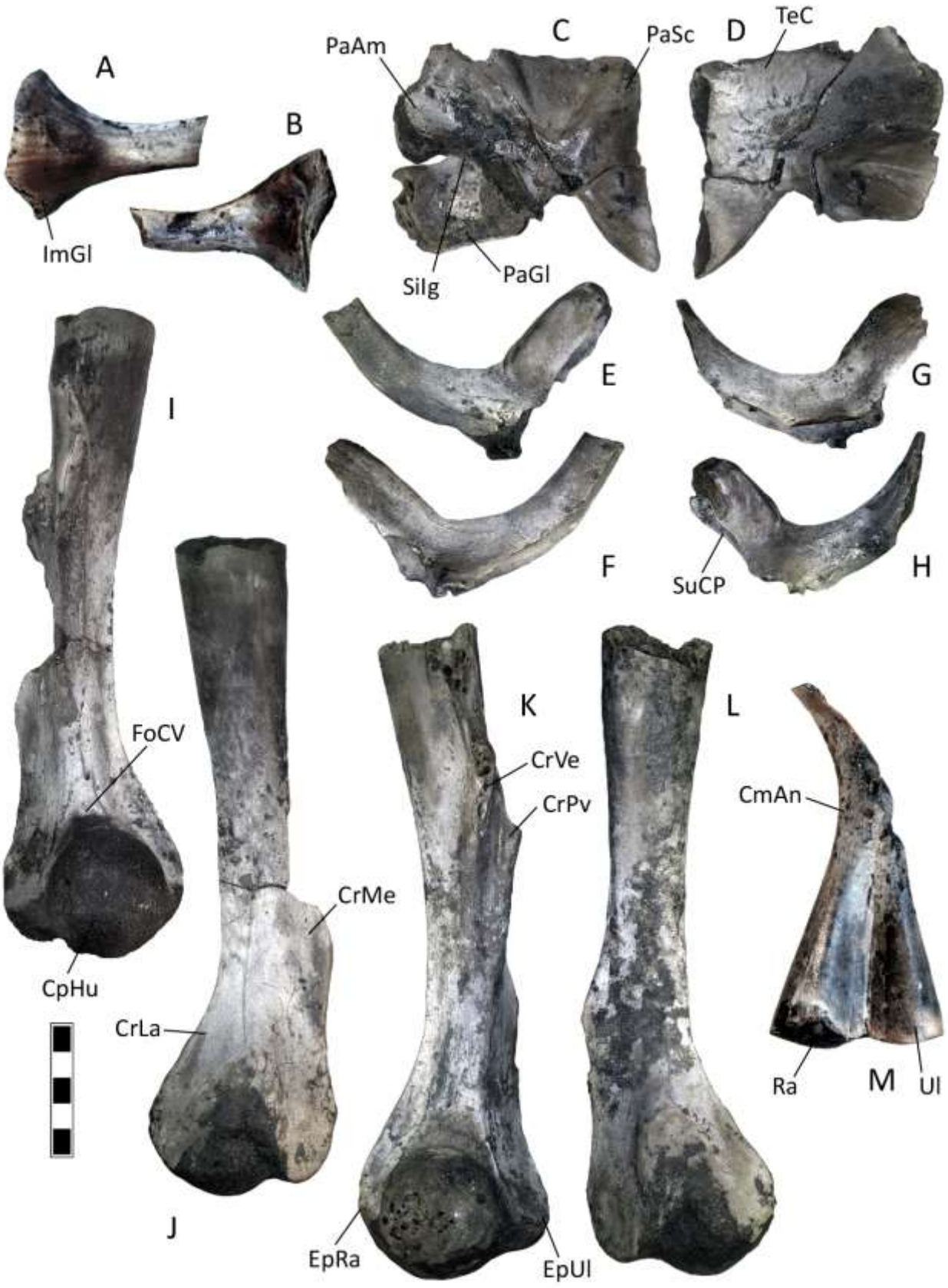

A
B
ImGl
C
PaAm
PaSc
Silg
PaGl
D
TeC
E
F
G
H
SuCP
I
FoCV
CpHu
J
CrLa
CrMe
K
CrVe
CrPv
EpRa
EpUl
L
CmAn
Ra
M
Ul

Figure 11

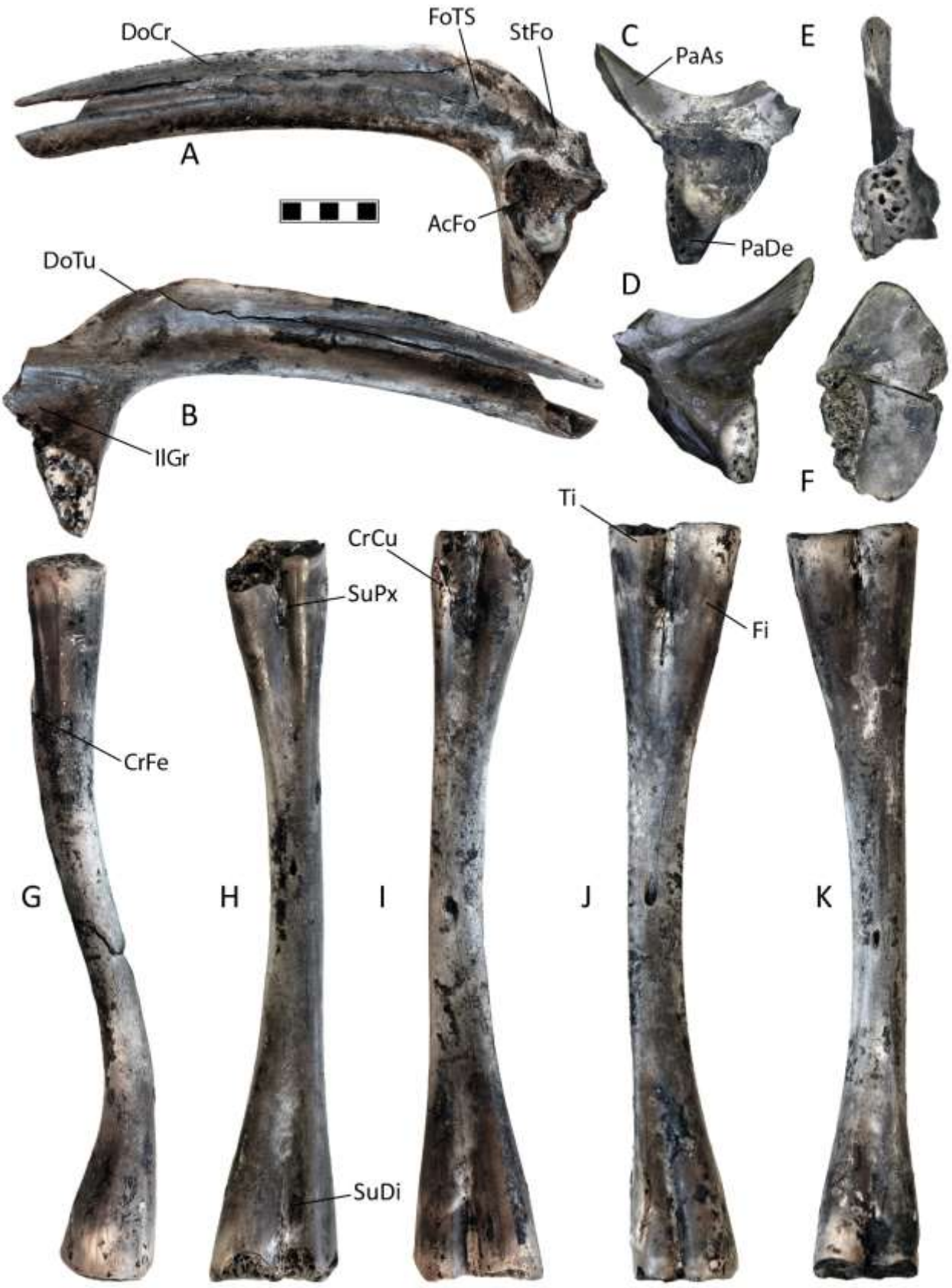

DoCr
FoTS
StFo
A
AcFo
C
PaAs
PaDe
E
DoTu
B
IlGr
D
F
Ti
CrCu
SuPx
Fi
CrFe
G
H
I
J
K
SuDi

Figure 12

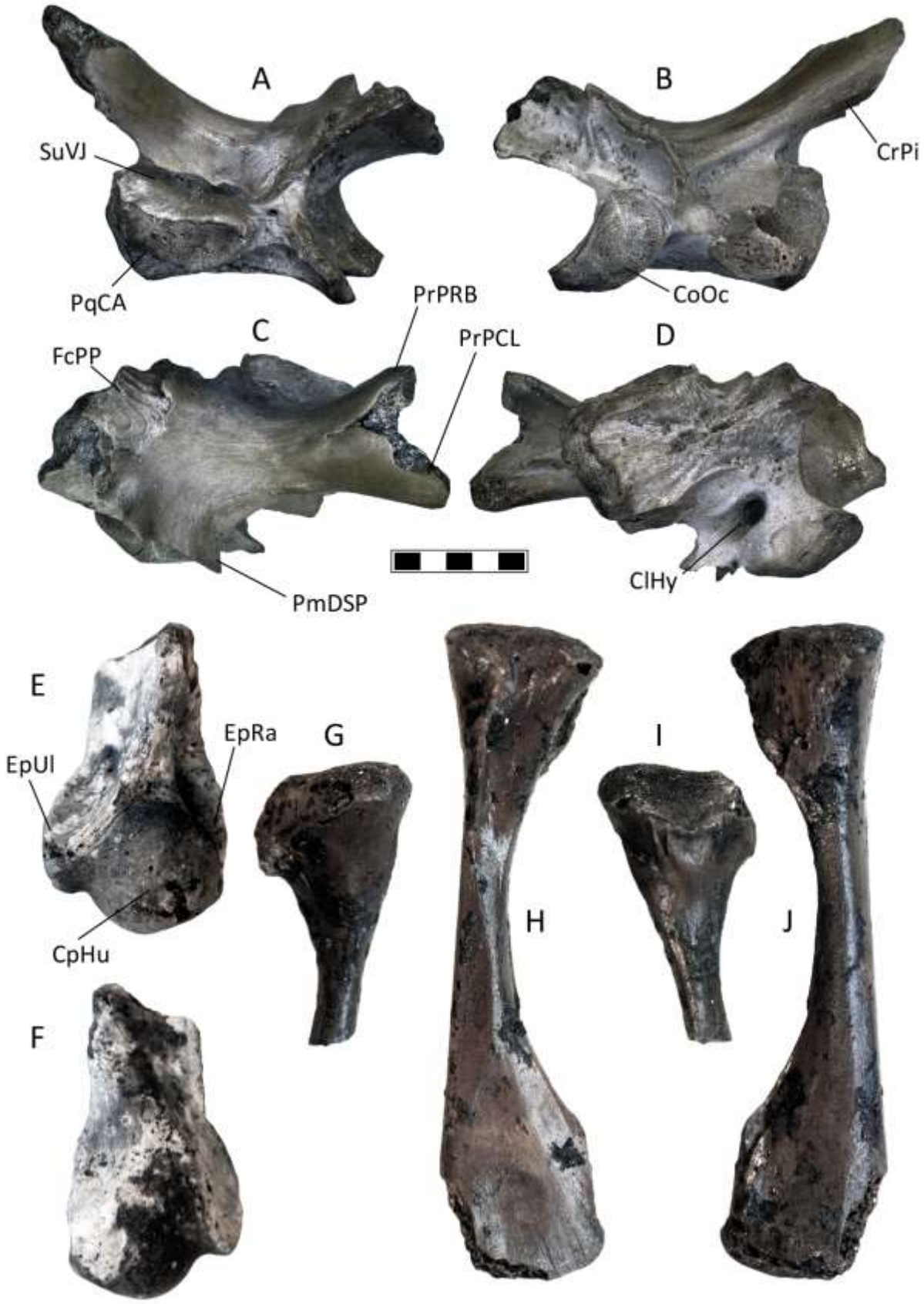

A
SuVJ
PqCA
B
CrPi
CoOc
C
PrPRB
PrPCL
FcPP
PmDSP
D
ClHy
E
EpRa
EpUl
CpHu
F
G
H
I
J

Figure 13

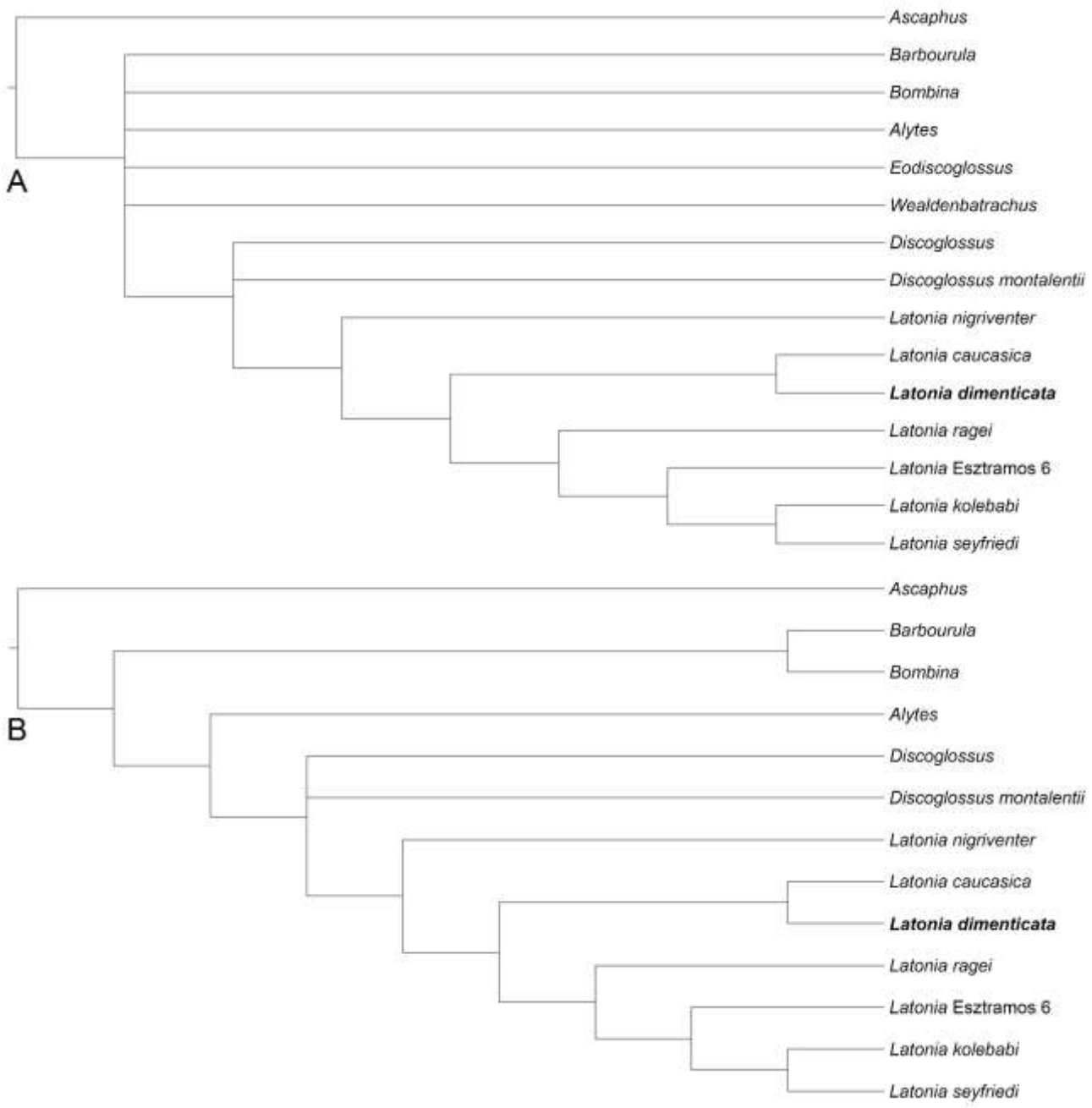

A
Ascaphus
Barbourula
Bombina
Alytes
Eodiscoglossus
Wealdenbatrachus
Discoglossus
Discoglossus montalentii
Latonia nigriventer
Latonia caucasica
Latonia dimenticata
Latonia ragei
Latonia Esztramos 6
Latonia kolebabi
Latonia seyfriedi
B
Ascaphus
Barbourula
Bombina
Alytes
Discoglossus
Discoglossus montalentii
Latonia nigriventer
Latonia caucasica
Latonia dimenticata
Latonia ragei
Latonia Esztramos 6
Latonia kolebabi
Latonia seyfriedi

Figure 14

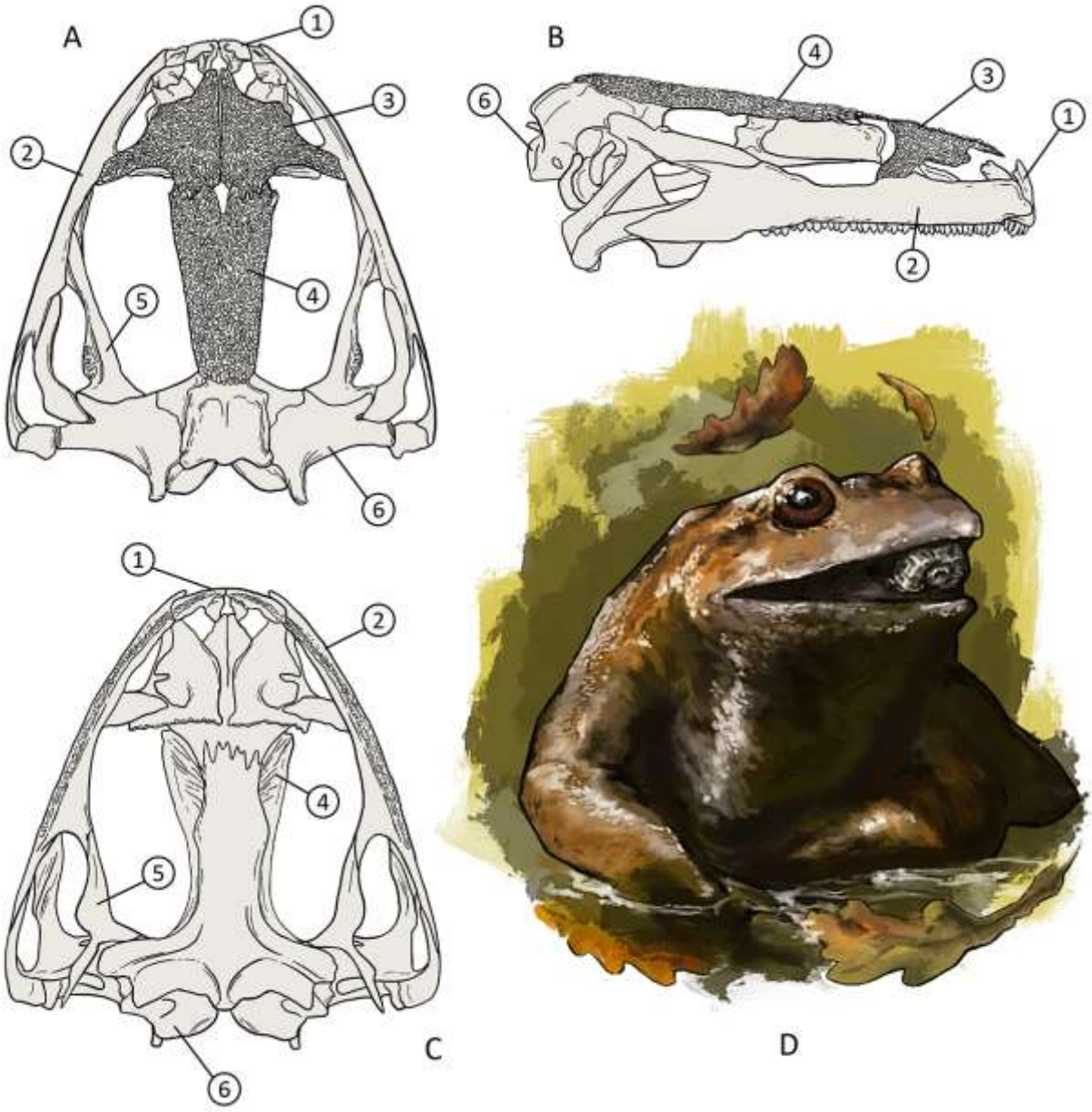


Figure 15